Dr-2112

ANL-75-42

ANL-75-42

274
4-1-76

USE OF COMPOUND PARABOLIC CONCENTRATOR FOR SOLAR ENERGY COLLECTION

by

Ari Rabl, Vaclav J. Sevcik,
Raymond M. Giugler, and Roland Winston

MASTER

U of C-AUA-USERDA

ARGONNE NATIONAL LABORATORY, ARGONNE, ILLINOIS

Prepared for the U. S. ENERGY RESEARCH
AND DEVELOPMENT ADMINISTRATION
under Contract W-31-109-Eng-38

DISCLAIMER

Printed in the United States of America
Available from
National Technical Information Service
U. S. Department of Commerce
5285 Port Royal Road
Springfield, Virginia 22161
Price: Printed Copy $5.50; Microfiche $2.25

Distribution Category:
Solar Thermal (UC-62)

ANL-75-42

ARGONNE NATIONAL LABORATORY
9700 South Cass Avenue
Argonne, Illinois 60439

USE OF COMPOUND PARABOLIC CONCENTRATOR FOR SOLAR ENERGY COLLECTION

by

Ari Rabl, Vaclav J. Sevcik,
Raymond M. Giugler, and Roland Winston

Progress Report for the Period
July—December 1974

THIS PAGE

WAS INTENTIONALLY

LEFT BLANK

TABLE OF CONTENTS

TABLE OF CONTENTS

LIST OF FIGURES

LIST OF FIGURES (cont)

LIST OF TABLES

THIS PAGE
WAS INTENTIONALLY
LEFT BLANK

THIS PAGE

WAS INTENTIONALLY

LEFT BLANK

ATURE

Symbol	Description
$\langle n \rangle_o$	Average number of reflections for full CPC, for radiation outside acceptance angle
$\langle \bar{n} \rangle_i$	Average number of reflections for truncated CPC, for radiation that can get from S to L
$\langle \bar{n} \rangle_o$	Average number of reflections for truncated CPC, for radiation that cannot get from L to S
$\langle \bar{n} \rangle_\theta$	Average number of reflections for truncated CPC, for radiation inside acceptance angle
Nu	Nusselt number
$P_i(n)$	Probability that radiation inside acceptance angle makes n reflections when it passes through CPC
$P_o(n)$	Probability that radiation outside acceptance angle makes n reflections when it passes through CPC
Pr	Prandtl number
q	Heat transfer (in $W\ cm^{-2}$ or $Btu\ ft^{-2}\ hr^{-1}$)
R	Thermal resistance
Re	Reynolds number
S	Insolation (direct plus diffuse), or circumference of a tube receiver
T	Temperature (in ^oK or ^oR)
T_{air}	Ambient air temperature
T_{sky}	Radiation temperature of sky
ΔT	Temperature difference
$U = 1/R$	Thermal conductance [in $W\ cm^{-2}(^oK)^{-1}$ or $Btu\ ft^{-2}\ hr^{-1}(^oF)^{-1}$]
v	Wind speed
β	Volume coefficient of expansion
γ	Fraction of insolation S that is accepted by CPC

The subscripts S, R, and L refer to absorber (small), reflector, and aperture (large); for example, the concentration is $C = A_L/A_S$, the ratio of aperture to absorber area, and q_{SR} is the radiative heat transfer from the absorber to the reflector. Barred quantities refer to a truncated CPC; the concentration of a truncated CPC trough, for example, is $C = \bar{A}_L/A_S = \ell/s$.

Symbol	Description
A	Area
a_{out}	Fraction of the radiation emitted by L that cannot get to S, even if the mirrors were perfect
C	Concentration
d_1	Diameter of entrance pupil
d_2	Diameter of exit pupil
f	Focal length of parabola
$f_d = f_d(\varepsilon_R)$	Fraction of the radiation emitted by R that goes to S
$f_o = f_o(\varepsilon_R)$	Fraction of the radiation emitted by R that hits L outside the acceptance angle
$f_u = f_u(\varepsilon_R)$	Fraction of the radiation emitted by R that hits L inside the acceptance angle
F_{SL}	Shape factor for radiation going from S to L
g	Acceleration due to gravity
Gr	Grashof number
h	Height of CPC
k	Thermal conductivity
k_x, k_y, k_z	Direction cosines of light rays. These are projections of the ray directions along the x, y, and z coordinate axes. In the text, $\underset{\sim}{k}$ is also used to denote the direction of the extreme ray accepted by the concentrator.
ℓ	Width of aperture
n	Index of refraction
$\langle n \rangle_i$	Average number of reflections for full CPC, for radiation inside acceptance angle

THIS PAGE

WAS INTENTIONALLY

LEFT BLANK

NOMENCLATURE

Symbol	Description
$\varepsilon = 1 - \rho$	Emissivity
$\varepsilon_{Ri} = 1 - \rho_{Ri}$	Effective absorptivity of CPC for radiation inside acceptance angle
$\varepsilon_{Ro} = 1 - \rho_{Ro}$	Effective absorptivity of CPC for radiation outside acceptance angle
η	Collector efficiency
$\rho = 1 - \varepsilon$	Reflectivity
$\rho_{Ri} = 1 - \varepsilon_{Ri}$	Effective "reflectivity" (transmissivity) of CPC for radiation inside acceptance angle
$\rho_{Ro} = 1 - \varepsilon_{Ro}$	Effective "reflectivity" of CPC for radiation outside acceptance angle
τ	Transmissivity of cover
θ	Acceptance half angle of CPC
θ'	Angle of incidence of a particular ray
θ_{max}	Maximum divergence (half-angle) of a light beam; also, the angular acceptance (half-angle) of a collector.

USE OF COMPOUND PARABOLIC CONCENTRATOR FOR SOLAR ENERGY COLLECTION

by

Ari Rabl, Vaclav J. Sevcik, Raymond M. Giugler, and Roland Winston

ABSTRACT

The joint team of Argonne National Laboratory (ANL) and the University of Chicago is reporting their midyear results of a proof-of-concept investigation of the Compound Parabolic Concentrator (CPC) for solar-energy collection. The CPC is a nonimaging, optical-design concept for maximally concentrating radiant energy onto a receiver. This maximum concentration corresponds to a relative aperture (f/number) of 0.5, which is well beyond the limit for imaging collectors. We have constructed an X3 concentrating flat-plate collector 16 ft^2 in area. This collector has been tested in a trailer laboratory facility built at ANL. The optical and thermal performance of this collector was in good agreement with theory. We have constructed an X10 collector (8 ft^2) and started testing. A detailed theoretical study of the optical and thermal characteristics of the CPC design has been performed.

I. INTRODUCTION

The CPC is a nonimaging optical-design concept for maximally concentrating radiant energy onto a receiver. The design incorporates a trough-like reflecting wall-light channel, which concentrates radiant energy by the maximum amount permitted by physical principles. This maximum concentration corresponds to a relative aperture (f/number) of 0.5, which is well beyond the limit for imaging collectors. Consequently, for concentrations up to about 10, diurnal tracking is not needed. The sun remains within the angular field of view of the stationary collector for one entire day (annual average of 8 hr). In one version of the design, radiation is collected over an entrance aperture of width d_1 and angular field view of $2\theta_{max}$, and concentrated onto an exit aperture of width d_2, where $d_1/d_2 = 1/\sin\theta_{max}$.

The profile curve of this collector consists of two distinct parabolas whose axes are inclined at angles $\pm\theta_{max}$; it should not be confused with the simple parabolic collector. In another version of the design, radiation is concentrated onto a tube receiver of very general shape. The concentration achieved is $d_1/S = 1/\sin\theta_{max}$, where S is the circumference of the tube. For certain applications, notably photovoltaic, the index of reflection (n) is greater at the exit than at the entrance ($n_2 > n_1$). The concentration is then increased by n_2/n_1. For some applications requiring very high concentrations, a conelike collector with the compound parabolic profile curve may be advantageous. All CPC designs are characterized by a large angular field of view and a high, uniform-throughput efficiency (the average number of reflections is < 1 for concentrations < 10). In many areas of solar-energy technology where optical concentration is indicated, the CPC design offers significant advantages, which may have important consequences. The flexibility of the concept permits advantageous application to many areas of solar-energy technology.

II. CONCENTRATING FLAT-PLATE COMPOUND PARABOLIC COLLECTORS

A. Introduction

A concentrating solar heater based on the compound parabolic design[1,2] has been constructed and tested at Argonne National Laboratory. A schematic drawing of the 4 ft x 4 ft collector is shown in Fig. 1. The principal characteristics of the collector are:

1. Concentration factor = 3.
2. Angular acceptance (full angle) = 38°. The large angular acceptance implies that biannual adjustment of the collector orientation is sufficient to accept direct solar radiation.

The modest concentration factor of 3 was chosen to permit efficient operation at 130°F above ambient temperature. Our experimental results from outdoor tests show good agreement with a detailed theoretical analysis (see Appendix A) and confirm the expected improvements in performance resulting from concentration.

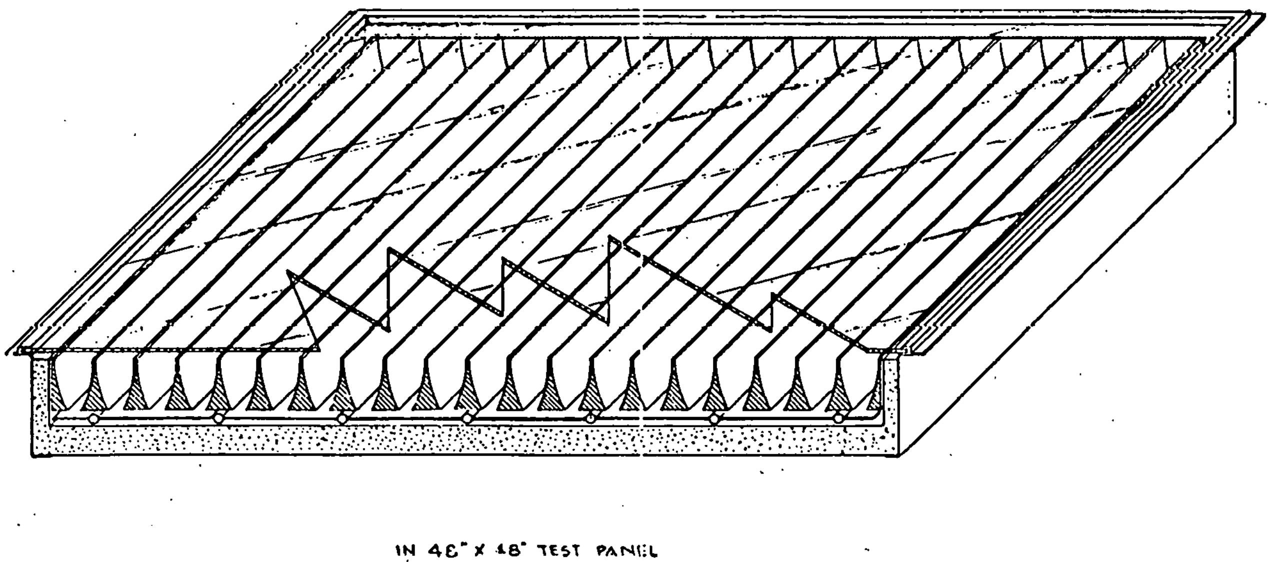

Fig. 1. X3 Collector Panel

B. Details of Construction

The collector consists of a black absorber plate, an array of 20 mirror bars with the compound parabolic profile shape, and a Plexiglas cover. The entire assembly is insulated on the back and sides and is contained in an aluminum box. The absorber plate is roll-bonded aluminum painted with a nonselective black having an absorptivity of 92%. The mirror bars (48 in. long by 3 in. high) were cast of epoxy resin from a master mold. The reflective surface is evaporated aluminum deposited on the sides and bottoms of the bars (reflectivity over the solar spectrum ≈ 88%). The Plexiglas cover (1/4 in. thick) transmits 86% of the solar spectrum.

C. Description of Experiments

Tests were conducted outdoors at Argonne National Laboratory during October-December 1974. The collector was mounted on a tilted platform approximately normal to solar noon. The incident solar radiation was monitored by three Epply pyranometers with the following geometries:

1. Horizontal.
2. On the tilted collector plane.
3. On the tilted collector plane, but masked for an angle of 38° (the acceptance angle of the collector).

The heat output of the collector was determined by flowing a 50% mixture of ethylene glycol and water and measuring the temperature rise in the collector and the flow rate. The flow rate was made sufficiently high (0.3-0.5 gpm) to maintain the collector fairly isothermal. To measure performance at elevated fluid temperature, the fluid was preheated. For diagnostic purposes, 22 temperatures of various points on the collector were monitored. All 24 temperatures were recorded on a single chart recorder. The three pyranometers were recorded on a separate chart recorder. Finally, wind speed and direction were recorded on separate charts. Our useful data were obtained only in clear-sky conditions with stable pyranometer readings. We required steady-state conditions for various temperatures on the collector. This especially applied to the epoxy mirror bars, which have large thermal capacity and can add or subtract heat from the system during transient conditions.

D. Experimental Results

1. Flat-plate Collector Without Concentrators

By removing the mirror-bar assembly, we are left with a simple flat-plate collector. Our data with this configuration serve to calibrate our data-taking system. A convenient form to present results is to plot the efficiency $\eta = Q_{out}/Q_{in}$ against $\Delta T/S$, where

Q_{out} = heat extracted by the fluid,

Q_{in} = SA,

$\Delta T = T_C - T_A$,

S = solar insolation (Btu $hr^{-1}ft^{-2}$),

A = collector window area (= 16.67 ft^2),

T_C = average collector-plate temperature,

and

T_A = ambient temperature.

One expects an approximately linear plot in these variable. This is shown in Fig. 2. The relevant parameters are the intercept at $T_C \rightarrow T_A$ and the slope. From these, one infers the no-thermal loss efficiency $\eta(0)$ = 80% and the heat-loss coefficient U = 1.0 Btu $hr^{-1}ft^{-2}(^{o}F)^{-1}$.

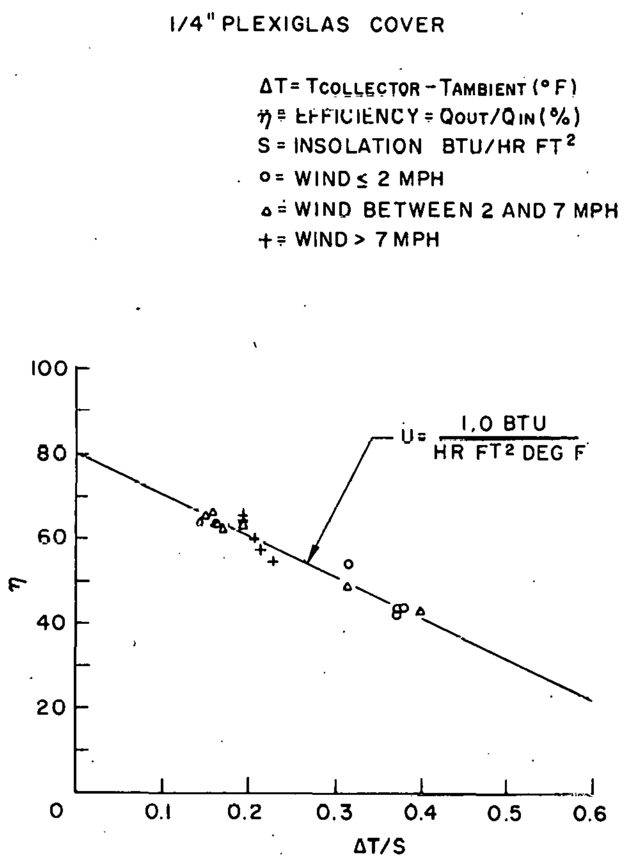

Fig. 2. Measured Efficiency of 4 ft x 4 ft Flat-plate Collector without Concentrators.

2. Concentrating Flat-plate Collector

A plot of our data with the mirror assembly in place is shown in Fig. 3. In this plot, we have divided by the insolation S measured by the masked pyranometer in order to make the data independent of atmospheric haze, and the area A = 15.36 ft^2 (8% of the window is obscured by the mirror assembly). From this we infer $\eta'(0)$ = 80% and the heat-loss coefficient U' = 0.65 Btu $hr^{-1} ft^{-2}(^{o}F)^{-1}$. The effect of concentration on suppressing heat loss is clear by comparing Figs. 2 and 3. To convert these to more useful values, we note that on a clear day the masked pyranometer detects 92% of the total insolation. The area for heat loss to the collector is 16.67 ft^2. The converted values are $\eta(0)$ = 74% and U = 0.60 Btu $hr^{-1}ft^{-2}(^{o}F)^{-1}$.

To compare our findings with theory, we must know the back and edge thermal-loss coefficient of our collector box. We have measured this by covering the front of the collector with 6 in. of Styrafoam plus 1.5 in. of Fiberglas and measuring the heat loss. For this configuration (see Fig. 4), we obtain U = 0.32. Allowing for the heat leak of even this thick front insulation, we estimate $U_{BOX} \approx$ 0.20 to 0.25. We conclude that the threefold concentrating collector is characterized by

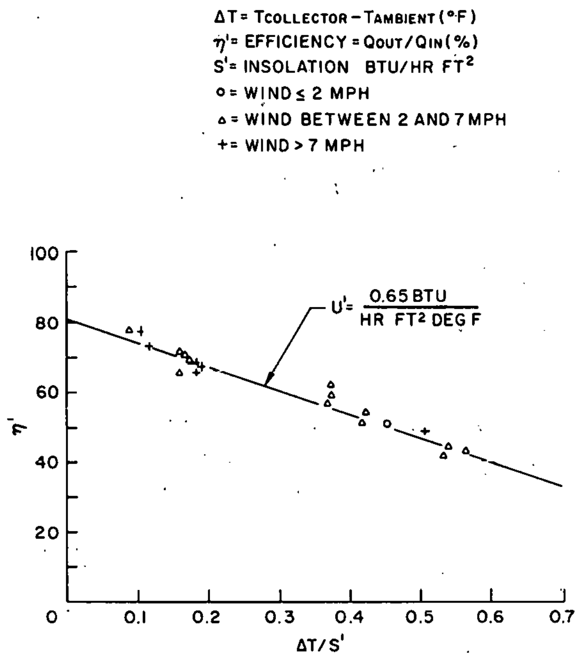

Fig. 3. Measured Efficiency of X3 Concentrating Collector.

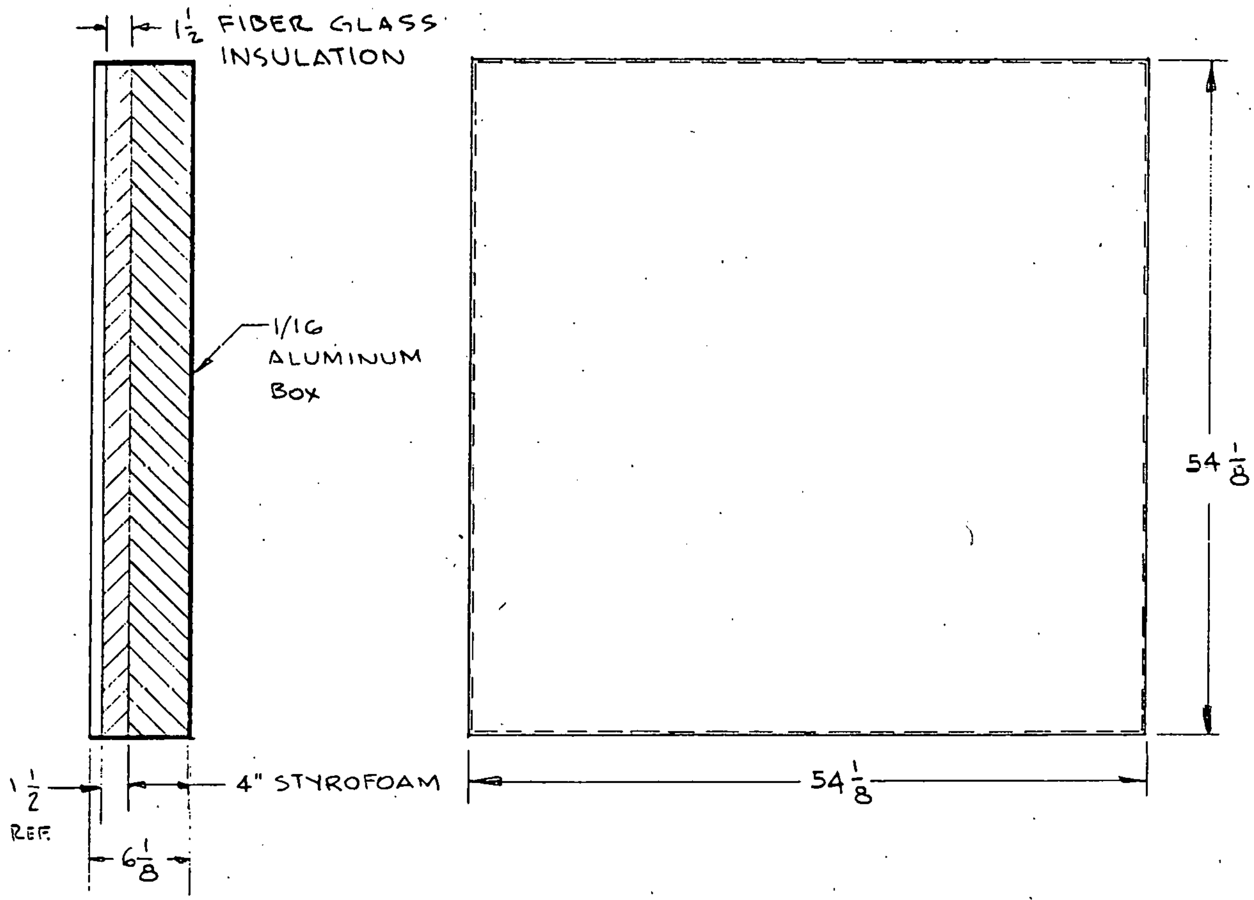

Fig. 4. Front-cover Insulation Used for Measuring Losses through Back and Sides of Collector.

$$\eta(0) = 74\%$$

and

$$U_{Front} = 0.35 \text{ to } 0.40.$$

This U_{Front} value (see Sec. III) is in good agreement with the result $U_{Front} \approx 0.40$ calculated by Kreider.

3. Angular Acceptance

The theoretical angular acceptance of a X3 CPC is an elliptic cone of 38 x 180° and should require no tracking between the equinox and the solstice. To check diurnal acceptance, we took data up to $3\frac{1}{2}$ hr away from solar noon. Figure 5 shows that Q_{out} is comparable with the cosine decrease of projected frontal area. In this plot, ΔT was fairly small ($\approx 55^oF$), so that heat loss is small. To check the seasonal acceptance, we took data with the collector oriented at 50° from vertical, during winter solstice (solar angle 65° from vertical). No decrease in efficiency was observed. In fact, this measurement is plotted as one of the largest ΔT data points in Fig. 3.

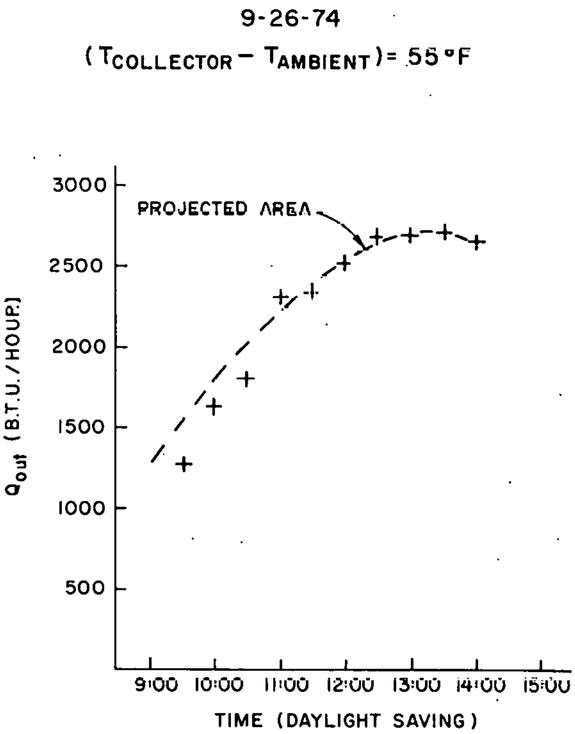

Fig. 5. Heat Output on a Clear Day.

E. Conclusions and Recommendations

The X3 CPC we have tested is characterized by an optical efficiency $\eta(0) = 74\%$ of total clear-sky radiation and a frontal heat loss $U_F = 0.35$ to 0.40 Btu $hr^{-1}ft^{-2}(^oF)^{-1}$. A practical collector would have a more trans-

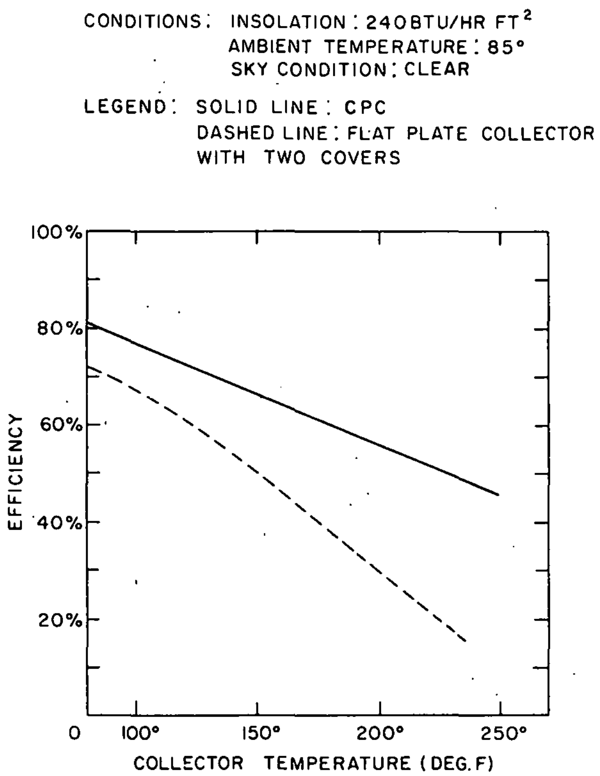

Fig. 6. Expected Performance of X3 CPC Concentrating Flat Plate.

parent cover (1/8 in. glass) and improved back insulation. Extrapolating our results to a collector with U = 0.50 and $\eta(0)$ = 80% would give the thermal performance shown in Fig. 6. Such performance would be useful for space-conditioning applications in a temperature range in which flat-plate collectors are marginal (130°F above ambient). In the present CPC, the absorber area is as large as the frontal area, with the mirror bars acting as radiation shields. We will test a version of the X3 CPC with the absorber area one-third the frontal area. This should produce improved thermal performance without reducing the optical performance.

III. OPTICAL AND THERMAL PROPERTIES OF COMPOUND PARABOLIC CONCENTRATORS

The optical and thermal properties of compound parabolic collectors have been extensively investigated during this reporting period. The results have been accepted for publication by Solar Energy[7], and the abstract of the paper is presented below:

> Compound Parabolic Concentrators (CPC) are relevant for solar energy collection because they achieve the highest possible concentration for any acceptance angle (tracking requirement). The convective and radiative heat transfers through a CPC have been calculated, and formulas for evaluating the performance of solar collectors based on the CPC principle are presented. A simple analytic technique for calculating the average number of reflections for radiation passing through a CPC was developed; this information is necessary for computing optical losses. In most practical applications, a CPC will be truncated because a large portion of the reflector area can be eliminated without seriously reducing the concentration. The effects of this truncation are described explicitly. The paper includes many numerical examples, displayed in tables and graphs, which should be helpful in designing CPC solar collectors.

APPENDIX A

PERFORMANCE STUDY OF THE COMPOUND PARABOLIC CONCENTRATOR SOLAR COLLECTOR

1. Summary

a. Purpose and Scope

The purpose of this study is to provide Argonne National Laboratory with a computer model of the Compound Parabolic Concentrator (CPC) solar collector. The study predicts performance for a single section of the CPC collector for three specific geometries defined by ANL. The model includes all first-order radiative and convective heat-transfer mechanisms. Optical data from ANL are used to describe the reflection properties of the CPC.

b. General Results

(1) The CPC collector performs well with one glass cover and fluid flow rates above a minimum value dependent upon collector area and concentration ratio.

Performance is better than that for a flat-plate collector with the same flow rate and inlet condition.

(2) The most important parameters governing collector performance for a given orientation are:

Mirrored surface reflectance.
Concentration ratio.
Working-fluid flow rate.
Radiation-surface properties of absorber.
Insolation level.

(3) The computer program developed for the present study can easily be integrated into a complete solar-building climate-control model including storage and building energy-demand elements.

c. Quantitative Conclusions

(1) Collector efficiencies of 40-50% for a nonselective absorber are easily achievable for concentration ratios in the range 3-10.

(2) A selective absorber surface will improve collector efficiency from 2 to 10% over the levels in (1) above.

(3) For the three geometries studied, efficiency gains are small for fluid flow rates beyond 20 lb/hr.

(4) For year-round use, the collector should be repositioned at least twice annually to favor the winter and summer sun angles.

(5) Collector efficiency falls off to 50% if its maximum value for insolation levels below 0.5 langley/min and for hour angles greater

than 55° under typical ambient climatic conditions.

(6) Subatmospheric wet steam used as a working fluid will result in better performance than liquid water at the same inlet temperature.

2. Introduction

The CPC is a nontracking solar collector consisting of two sections of a parabola of second degree located symmetrically about the collector mid plane. The two sections form a single curvature, or trough-like solar concentrator with an angular acceptance of 2 x θ_{max} as shown in Fig. A.1. The acceptance depends upon the ratio of aperture and absorber areas and can be quantified by the relationship

$$\theta_{max} = \sin^{-1}(W_a/W_e). \qquad (A.1)$$

The collector is oriented in an east-west direction and is tilted toward the south at an angle β from the horizontal plane. When the angle γ $(=|\pi/2 - \beta - C|)$ is less than θ_{max}, the CPC accepts both direct and diffuse components of sunlight. When the angle γ is greater than θ_{max}, the CPC accepts only diffuse skylight over a portion of the aperture equal to the absorber area.

The depth of the collector h_{coll} depends on the concentration ratio CR as given in

$$\frac{h_{coll}}{W_a} = (CR + 1)/2 + \sqrt{CR^2 - 1} . \qquad (A.2)$$

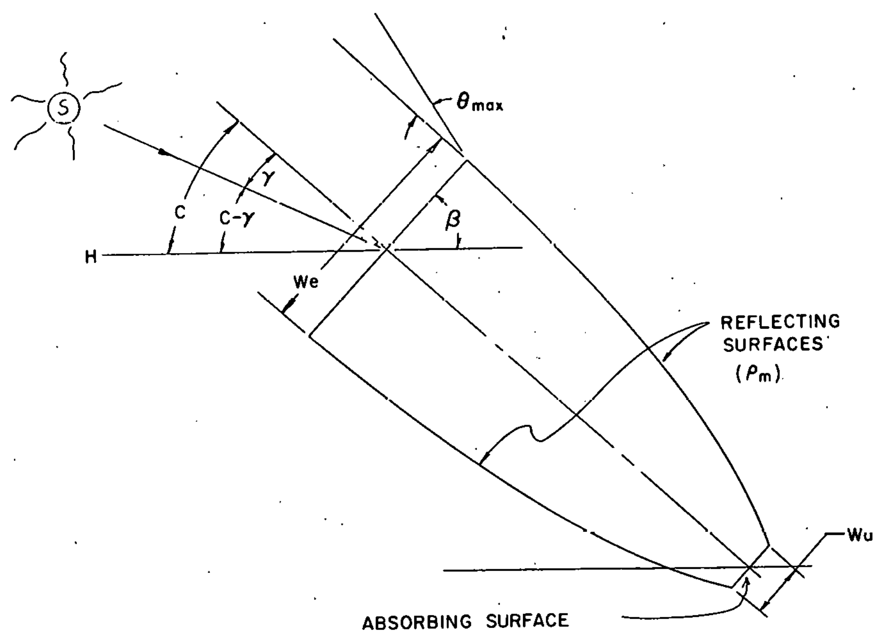

Fig. A.1. Schematic Diagram of Compound Parabolic Concentrator (CPC)

In practice, it has been found advantageous to use a smaller value of h_{coll} than that dictated by Eq. A.2. The advantage of such a truncation is that, for a significantly reduced mirrored surface, the angular acceptance is reduced only slightly for a given concentration ratio. In addition, the greatest number of reflections of sunlight between the aperture and the absorber would take place in the truncated region. Removing this high-reflectance density zone reduces the number of reflections of normally incident incoming light by about 20%. The present study considers only the less costly truncated collector.

Three relatively low values of concentration ratio CR have been considered in the present study. The CR values and collector dimensions are shown in Table A.1.

TABLE A.1. Important Collector Dimensions

Nominal Concentration Ratio	Aperture Width in.	Absorber Width in.	Height in.	Length ft.
3	27.7	9.44	36	4
5	18.0	3.56	36	4
10	12.0	1.20	36	4

Although mathematical models are amenable to performance prediction by means of dimensionless variables (e.g., efficiency η as a function of CR), this approach has not been used exclusively in this work. Instead, the three specific geometries of Table A.1 were used with dimensional parameters and outputs.

The primary parameters that determine CPC performance are:

a. CR, concentration ratio.
b. $\dot{m}$, working-fluid throughflow rate.
c. β, collector tilt.
d. ρ_m, mirror reflectance.
e. n, number of glass covers (zero or one).
f. G_s, insolation.
g. Radiation surface properties of reflector and absorber.

The manner in which these variables interact is described in Sec. 3. Four basic configurations have been analyzed.

a. Uncovered collector, water-cooled.
b. Uncovered collector, steam-cooled.
c. Covered collector, water-cooled.
d. Covered collector, steam-cooled.

The results of the model runs are given in Sec. 4.

In creating the CPC mathematical model, we used the philosophy of constructing it so that it could easily be integrated into a total system model in the future, i.e., into an integrated model of a collector, a storage unit, and a building with specific energy demands. It is the total system study, not the component-by-component study, that enables the engineer to determine optimal component specifications.

3. Analysis

Hinterberger and Winston[5], Winston[3,11], and Sevcik et al.[2] have described the optical characteristics of the CPC collector in detail. The purpose of the present work is to complete the collector-performance picture by coupling thermodynamic and sun-earth geometric relationships to the preceding optical analyses. A detailed analysis of convective and radiative processes within the collector is used to predict total collector performance.

The energy exchanges between the absorber, the collector mirror, and the collector cover are complex. They include radiative exchanges and forced- and natural-convection exchanges. To make the system tractable for analysis, some higher-order effects can be neglected so that the analysis is simplified without loss of any important, first-order effects. It has therefore been assumed that the radiative processes can be modeled by a dual-band method consisting of a long-wavelength (IR) band in which all lower-temperature radiation occurs and a short-wavelength (UV, e.g., ultraviolet + visible) band in which solar-radiation exchanges occur. Surface radiation properties, except for those of the collector cover, are assumed angle-independent and constant. Free and forced-convection processes are represented by empirical correlations. The effects of polarization of sunlight by atmospheric scattering are not considered, since insufficient data are available with which to quantify this phenomenon.

The absorber has not been modeled in great detail to permit flexibility in using any absorber design in the future. It is represented parametrically by five quantities:

a. $\alpha_{a,uv}$, surface absorptance for UV.
b. $\alpha_{a,d}$, surface absorptance for diffuse UV (skylight).
c. $\varepsilon_{a,IR}$, surface emittance.
d. $\dot{m}$, absorber fluid throughflow (water or steam).
e. A_a, absorber area (projected parallel to aperture plane).

Effects of reflecting-surface errors have not been considered, since errors in the transverse or longitudinal planes, unless very large, will not cause insolation rejection; only the point of impingement on the absorber will change from the ideal optics location. Because of a similar argument, the divergence angle of the sun's disk is ignored. The ends of the collector trough plane were assumed to be mirrored.

In a low-temperature, uniform-flux concentrator, the longitudinal variations of cover and absorber temperature need not be considered in either continuous or finite-difference form. Detailed computer studies by ECS, Inc., of a solar collector similar to the CPC have shown that calculations using a single average temperature for cover and absorber will give performance results within the accuracy of parametric inputs when compared to calculations using a temperature distribution on the cover and absorber.

a. Heat Fluxes

The following heat fluxes, all based upon a unit absorber area, are considered:

(1) $Q_{uv,a}$ (UV wavelength region), direct solar radiation absorbed by the absorber both directly and indirectly after reflection from the envelope.

(2) $Q_{uv,e}$ (UV wavelength region), direct solar radiation absorbed by the cover both directly and indirectly after reflection from the absorber.

(3) $Q_{d,a}$ (UV wavelength band), diffuse solar radiation absorbed by the absorber.

(4) $Q_{d,e}$ (UV wavelength band), diffuse solar radiation absorbed by the cover.

(5) $Q_{ir,ae}$ (IR wavelength band), radiative exchange between the absorber and cover.

(6) $Q_{e,sky}$ (IR wavelength band), radiative exchange between the cover and the environment.

(7) $Q_{c,ae}$, convective exchange between the absorber and the cover.

(8) $Q_{c,e}$, convective loss from cover to the environment.

(9) Q_o, useful heat extraction.

The heat loss through the collector and absorber outer walls can be made very small by proper insulation and is therefore of higher order than the above nine heat fluxes and can be ignored.

The heat-flux terms are given in the following equations with acronymic subscripts:

$$Q_{uv,a} = G_s \cos i \; \tau_{e,uv}(i) \; \rho_m^r \; \alpha_{a,uv}(1 + \rho_{a,uv}\rho_{e,uvd}), \tag{A.3}$$

$$Q_{uv,e} = G_s \cos i \; [\alpha_{e,uv}^{(i)} + \tau_{e,uv}^{(i)}\rho_m^r\rho_{a,uv}\alpha_{e,uvd}](W_e/W_a), \tag{A.4}$$

$$Q_{d,a} = X_d\tau_{e,d}\alpha_{a,d}, \tag{A.5}$$

$$Q_{d,e} = X_d\alpha_{e,d}(W_e/W_a), \tag{A.6}$$

$$Q_{ir,ae} = \varepsilon_{eff}\sigma(T_a^4 - T_e^4), \tag{A.7}$$

$$Q_{e,sky} = \varepsilon_{e,ir}\sigma(T_e^4 - T_{sky}^4)(W_e/W_a), \tag{A.8}$$

$$Q_{c,ae} = h_{c,ae}(T_a - T_e), \tag{A.9}$$

and

$$Q_{c,e} = h_{c,e}(T_e - T_\infty)(W_e/W_a), \tag{A.10}$$

in which

$$X_D = 0.78 + 1.07\alpha + 6.17CC \text{ (diffuse skylight magnitude)},$$

$$\sin\alpha = \sin\delta_s \sin L + \cos\delta_s \cos L \cos h,$$

$$\cos i = \sin\delta_s \sin(L - \beta) + \cos\delta_s \cos(L - \beta)\cos h,$$

$$T_{sky} = 0.914T_\infty,$$

$$h_{c,ae} = (1/h_{ca} + W_a/W_e h_{ce})^{-1},$$

$$h_{ca} \text{ or } h_{ce} = 0.54(k_f/W)(GrPr)^{1/4}$$ (h_{ca}, h_{ce} convection coefficients from absorber or cover to air entrapped in collector),

$$h_{c,e} = 0.54(k_f/W_e)(GrPr)^{1/4}$$ (calm environment, free convection),

and

$$h_{c,e} = C(k_f/L_c)(R_e^n - A)$$ (forced convection over cover; C,A,n in Ref. 12).

The effective emittance ε_{eff} contains cover and absorber radiation properties and geometric shape factors.[13] The angle-dependent cover transmittance $\tau_{e,uv}^{(i)}$ and absorptance $\alpha_{e,uv}^{(i)}$ for direct UV radiation are calculated from the equations of Stokes.[14] The viscosity and thermal-conductivity temperature dependence of air are represented by a power law in the mean film temperature for convective coefficient computations.

b. Energy Equations

The energy equations relate input energy terms to losses and to the useful output of the collector. The unknown quantities in the energy equations are Q_o, T_a, and T_e, for which there are three equations to be solved simultaneously. The absorber energy equation is

$$Q_{uv,a} + Q_{d,a} = Q_o + Q_{c,ae} + Q_{ir,ae}. \tag{A.11}$$

The cover energy equation is

$$Q_{uv,e} + Q_{ir,ae} + Q_{c,ae} + Q_{d,e} = Q_{e,sky} + Q_{c,e}. \tag{A.12}$$

The transport-fluid energy equation is (h_o,h_i - enthalpy)

$$h_o - h_i = Q_o A_a/\dot{m}. \qquad (A.13)$$

An order-of-magnitude analysis showed that the resistance offered to heat transfer for steam or water at the inner surface and in the wall of the absorber were of higher order than the external surface resistance. Consequently, the fluid and absorber temperatures are the same to lowest order. The energy-balance equations are solved in simultaneous iterative manner by computing T_e from Eq. A.12, Q_o from Eq. A.11, and h_o (or T_{ao}) from Eq. A.13. This iterative technique is continued until T_e, Q_o, and h_o (or T_{ao}) are known to 0.1%.

Collector efficiency η is defined as the system output, divided by maximum possible output, limited only by the second law of thermodynamics:

$$\eta = (Q_o A_a)/[A_e(G_s + X_D)]. \qquad (A.14)$$

4. The Computer Model

The analysis presented in the preceding section can be used to predict the performance of a CPC collector by means of a computer. This section describes the computer model CPCMOD and its method of operation.

The FORTRAN IV code consists of one main routine CPCMOD and four subroutines. The main routine CPCMOD reads in all data, performs the heat-transfer calculations, and prints out the results. Subroutine SHAPE computes ε_{eff}, the effective emittance for IR radiative exchange between the absorber and cover. Subroutine HCAE computes $h_{c,ae}$, the coefficient of convective exchange between the absorber and cover. Subroutine HCE computes $h_{c,e}$, the coefficient of convective exchange between the cover and the environment. Subroutine REFL determines the average number of reflections r that an entering beam at angle γ experiences between aperture and absorber. The main routine and all subroutines are listed in Sec. 7.

a. Structure of Input-data Deck

The input data contain all the parameters and initial values required for a unique solution of the equations along with certain computational parameters.

(1) TITLE card. The first card of the data deck is the card on which the title of the current run is entered in A10 format. If the first work of the title is STEAM, the working fluid is steam. For any other first word, the fluid is water.

(2) Control Card. For identifying the type of data, an integer from 1 to 9 is used in the first column of each data card in I1 format.

(3) Parametric Values. Up to seven parameters appear on each data card, each in F10 format as specified below for each data type.

(4) STOP Card. The last card of the data deck has the word STOP in the first four columns. This card terminates the run.

There are six data types, each of which must be identified by a digit 1-6 in the first column. The card following the six data types has a 9 in column one; this card causes the program to execute for the given input data. The data types are described below.

Type 1 Data

These data include:

GS, direct insolation (Btu $hr^{-1}ft^{-2}$).
WIND, average wind speed (knots).
XTINF, ambient temperature (^{o}F).
XPINF, ambient pressure (in. Hg).
DAY, day of year counted from January 1.
XLAT, latitude of collector (deg).
CC, average cloud cover index.

Type 2 Data

These data include:

AAUV, absorber UV absorptance.
EAIR, absorber IR emittance.
AAD, absorber skylight absorptance.

Type 3 Data

These data include:

REUVD, cover diffuse UV reflectance.
AEUVD, cover diffuse UV absorptance.
TG, cover material thickness (in.).
NR, cover index of refraction.
K, cover extinction coefficient ($in.^{-1}$).
TED, cover skylight transmittance.
AED, cover skylight absorptance.

Type 4 Data

These data include:

EEIR, cover IR emittance.
REIR, cover IR reflectance.

Type 5 Data

These data include:

LC, collector length (ft.).
XHCOLL, Collector height (in.).
RM, mirror reflectance.

CR, nominal concentration ratio.
XWE, aperture width (in.).
XWA, absorber width (in.).
XBETA, collector tilt (deg).

Type 6 Data

These data include:

XMDOT, working fluid flow rate (lb hr^{-1}).
XTAIN, working fluid flow inlet temperature (^{o}F).
DDT, calculation time increment (hr).

The assembly and contents of a typical deck of data cards are shown in Table A.2.

TABLE A.2. Content and Order of Input Cards for One Model Run

		Data Field (Column Numbers)					
1 2	12	22	32	42	52	62	Format
(TITLE CARD)							A5,7A10
1 GS	WIND	XTINF	XPINF	DAY	LAT	CC	I1,7F10.2
2 AAUV	EAIR	AAD					I1,3F10.2
3 REUVD	AEUVD	TG	NR	K	TED	AED	I1,7F10.2
4 EEIR	REIR						I1,2F10.2
5 LC	XHCOLL	RM	CR	XWE	XWA	XBETA	I1,7F10.2
6 XMDOT	XTAIN	DDT					I1,3F10.2
9	(Causes execution)						I1
S TOP	(Terminates run)						A4

More than one simulation can be made in one computer run. This is done by placing the decks of input cards in consecutive order. Data that are the same from one simulation to the next, are carried over automatically without the need to respecify. Each new data deck or partial deck must be preceded by a TITLE card. This feature of the program permits an entire parameter traverse (e.g., $\dot{m}$ or CR) to be made in one computer engagement.

b. Outputs

The first portion of output is simply a printout of the input data, a sample of which is shown in Fig. A.2. The computed output follows the input data. A unit of output consists of one line; the contents of each line are the values of the variables appearing at the head of each page of output.

```
CLIMATOLOGICAL DATA:
     DIRECT INSOLATION (BTU/HRSQFT):                300
     AVERAGE WIND SPEED (KNOTS):                      0
     AMBIENT TEMPERATURE (DEG F):                    30
     AMBIENT PRESSURE (IN HG):                       30
     DAY OF YEAR FROM JAN 1:                         81
     LATITUDE OF COLLECTOR (DEG):                  41.7
     AVERAGE CLOUD COVER INDEX:                       3

ABSORBER RADIATION PROPERTIES:
     ABSORBER UV ABSORPTANCE:                       .90
     ABSORBER IR EMITTANCE:                         .10
     ABSORBER SKYLIGHT ABSORPTANCE:                 .90

COLLECTOR COVER PROPERTIES:
     COVER DIFFUSE UV REFLECTANCE:                  .18
     COVER DIFFUSE UV ABSORPTANCE:                  .04
     COVER MATERIAL THICKNESS (IN):                .125
     COVER REFRACTIVE INDEX:                      1.520
     COVER EXTINCTION COEFFICIENT(/IN):            .130
     COVER SKYLIGHT TRANSMITTANCE:                  .77
     COVER SKYLIGHT ABSORPTANCE:                    .05
     COVER IR EMITTANCE:                            .88
     COVER IR REFLECTANCE:                          .05

COLLECTOR SPECIFICATIONS:
     COLLECTOR LENGTH (FT):                        4.00
     COLLECTOR HEIGHT (IN):                       30.00
     COLLECTOR REFLECTANCE:                         .85
     NOMINAL CONCENTRATION RATIO:                    10
     APERTURE WIDTH (IN):                         12.00
     ABSORBER WIDTH (IN):                          1.20
     COLLECTOR TILT (DEG):                         41.7

OPERATING AND COMPUTATIONAL PARAMETERS:
     FLOW RATE (LB/HR):                           15.00
     FLUID INLET TEMPERATURE:                       110
     TIME INCREMENT (HR):                            .5
```

Fig. A.2. Example Printout of Input Data.

The outputs are:

HOUR, time from solar noon (hr).
COLLECTION, delivery (Q_oA_a)(Btu hr^{-1}).
EFFICIENCY, $(Q_oA_a)/[A_e(X_D + G_s)]$.
INLET TEMP, inlet fluid temperature (°F).
OUTLET TEMP, outlet fluid temperature (°F).
COVER TEMP, cover temperature (°F).

A sample of output is shown in Fig. A.3.

PERFORMANCE RESULTS

HOUR	COLLECTION	EFFICIENCY	INLET TEMP	OUTLET TEMP	COVER TEMP
0.0	763	51.4	110.0	160.9	28.6
.5	756	51.0	110.0	160.4	28.5
1.0	735	49.9	110.0	159.0	28.3
1.5	700	47.8	110.0	156.7	27.6
2.0	652	45.0	110.0	153.5	27.3
2.5	590	41.1	110.0	149.3	26.6
3.0	513	36.3	110.0	144.2	25.8
3.5	423	30.4	110.0	138.2	24.6
4.0	320	23.3	110.0	131.3	23.7
4.5	206	15.3	110.0	123.7	22.5
5.0	90	6.8	110.0	116.0	21.2
5.5	-4	-.3	110.0	109.7	20.0

COLLECTION PERIOD TERMINATED - INCIDENCE ANGLE GREATER THAN 90 DEGREES

Fig. A.3. Example Printout of Model Output.

c. General

The important variables in the FORTRAN program are shown in Sec. 6 along with their equivalents in the symbolism used in Eqs. A.1-A.14. Computations are carried out from solar noon to sunset for any magnitude of time increment desired. When the model is integrated into a full system model, this feature is removed and calculations are carried out on an hourly basis using National Weather Service data.

5. Collector Performance

Performance of the CPC collector as modeled in CPCMOD depends upon specification of 34 different parametric inputs. The role of each parameter in collector performance can be traced by use of the computer model. In this section, the effects of the most important parameters are described by means of some demonstration computer runs. Any combination of the 34 parameters may be modeled, however. The most important parameters for a given working fluid are:

$\dot{m}$, fluid throughflow rate (lb hr^{-1});
CR, nominal concentration ratio (ratio of aperture to absorber area);
G_s, insolation (Btu $ft^{-2}hr^{-1}$);
n, number of covers (0 or 1);
$\alpha_{a,uv}$, absorber solar absorptance;

and

$\varepsilon_{a,ir}$, absorber IR emittance.

The effect of each parameter is described in summary fashion below for water as the fluid. The results for steam are similar and are not presented in detail. Unless otherwise specified, the following fixed values for the remaining parameters were used:

Wind = 0 knots,
T_∞ = 30°F,
p_∞ = 30 in. Hg,
Day = 81 (vernal equinox),
Latitude = 41.7° (Argonne, Ill.),
CC = 3,
$\alpha_{a,d}$ = 0.90,
$\rho_{e,uvd}$ = 0.18,
$\alpha_{e,uvd}$ = 0.04,
t_g = 0.125 in.,
n_r = 1.52,
k = 0.13 $in.^{-1}$,
$\tau_{e,d}$ = 0.77,
$\alpha_{e,d}$ = 0.04,
$\varepsilon_{e,ir}$ = 0.88,
$\rho_{e,ir}$ = 0.05
L_c = 4 ft,
h_{coll} = 36 in.,
ρ_m = 0.85 (specified by ANL),
β = 41.7° (= latitude),
T_{ai} = 110°F,

$$\Delta t = 0.5 \text{ hr},$$

and $\theta_{max} = 5^\circ$ for CR = 10

$= 11^\circ$ for CR = 5

$= 19^\circ$ for CR = 3

The average number of reflections r were determined by ANL using a Monte Carlo method.

a. Effect of Fluid Flow Rate

The effect of flow rate $\dot{m}$ on performance is shown in Figs. A.4-A.6 for CR = 3, 5, and 10. At flow rates greater than 15 lb hr^{-1}, the efficiency is nearly constant, except for CR = 3. All other things remaining constant, the fluid flow rate controls the outlet temperature. As $\dot{m}$ decreases below 15 lb hr^{-1}, efficiency suffers because of higher absorber temperature.

b. Effect of Concentration Ratio

The effect of concentration ratio CR is to improve performance by reducing the area from which heat loss occurs. However, in the CPC, increased CR results in increased reflection losses. If a selective surface is used to reduce IR losses from the absorber by 90%, the lowest concentration-ratio collector is the most efficient because of this reflection effect. The effect of CR is shown in Figs. A.4-A.6.

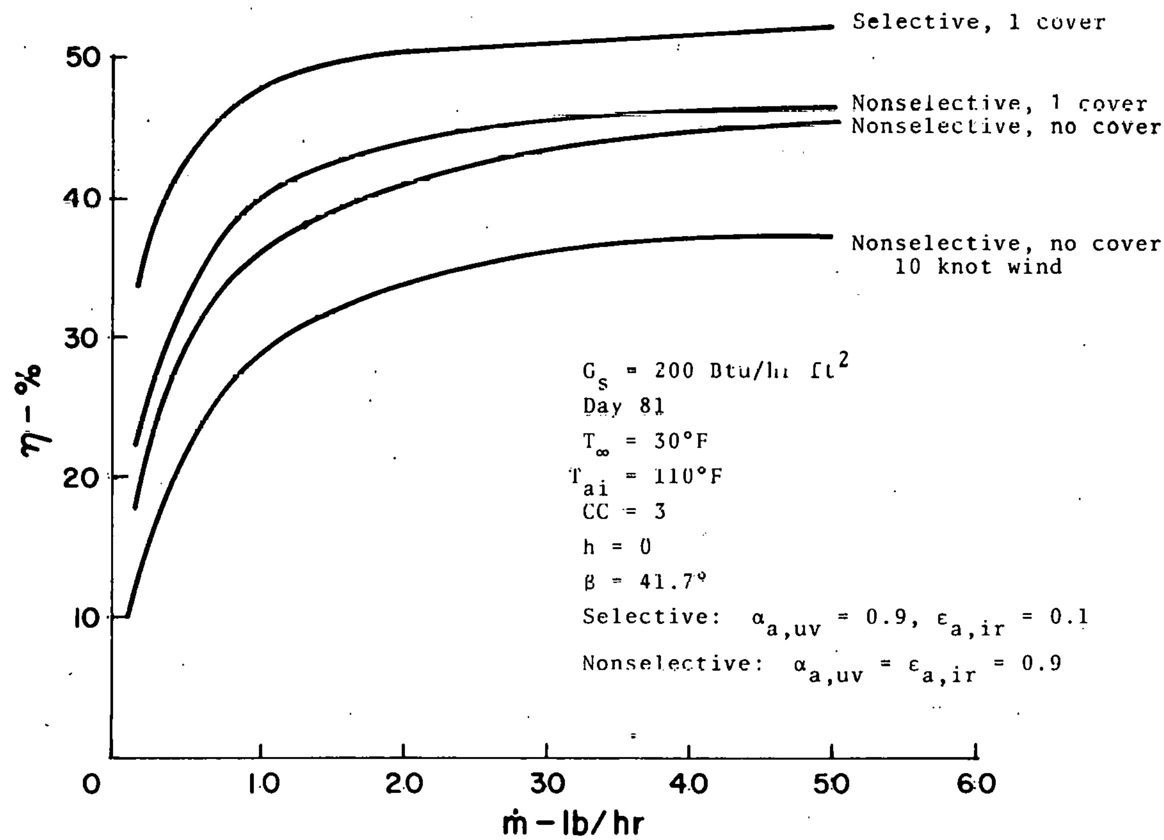

Fig. A.4. Midday Efficiency vs Flow Rate for CR = 3.

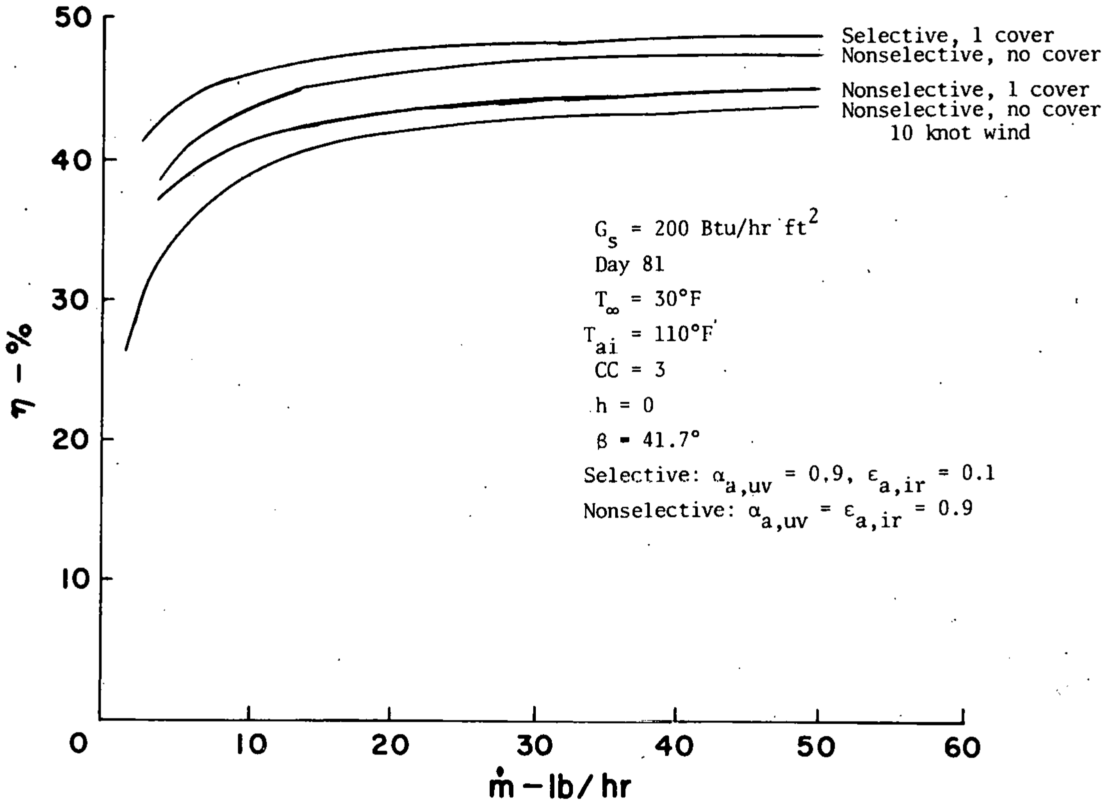

Fig. A.5. Midday Efficiency vs Flow Rate for CR = 5.

c. <u>Effect of Insolation</u>

Figure A.7 shows the effect of direct insolation G_s for a selected collector configuration. Efficiency drops off sharply for G_s < 125 Btu hr^{-1} ft^{-2}. This follows from the relative magnitude of losses and inputs. Losses depend primarily upon absorber temperature and do not vary with G_s. As a result, losses are <u>relatively</u> higher for lower insolation levels. This behavior is common to all solar collectors.

d. <u>Effect of Number of Covers</u>

The effect of using one glass cover or no glass cover is shown in Figs. A.4-A.6. The effect of a cover is a reduction in convection losses, but also an increase in insolation attenuation due to cover absorption and reflection. The effect of a cover varies with CR. For CR = 3, a cover is beneficial; for CR = 10, it is not. For CR = 5, it is beneficial when used with a selective surface, but is detrimental with a nonselective absorber surface. The curves in Figs. A.4-A.6 also show the effect of a 10-knot breeze on an uncovered collector. Performance of a collector without a convection shield suffers in any breeze above 0.5 knot. In practice, a cover would be used for any value of CR for performance and maintenance reasons. A cover serves as a dust shield in addition to its thermal function.

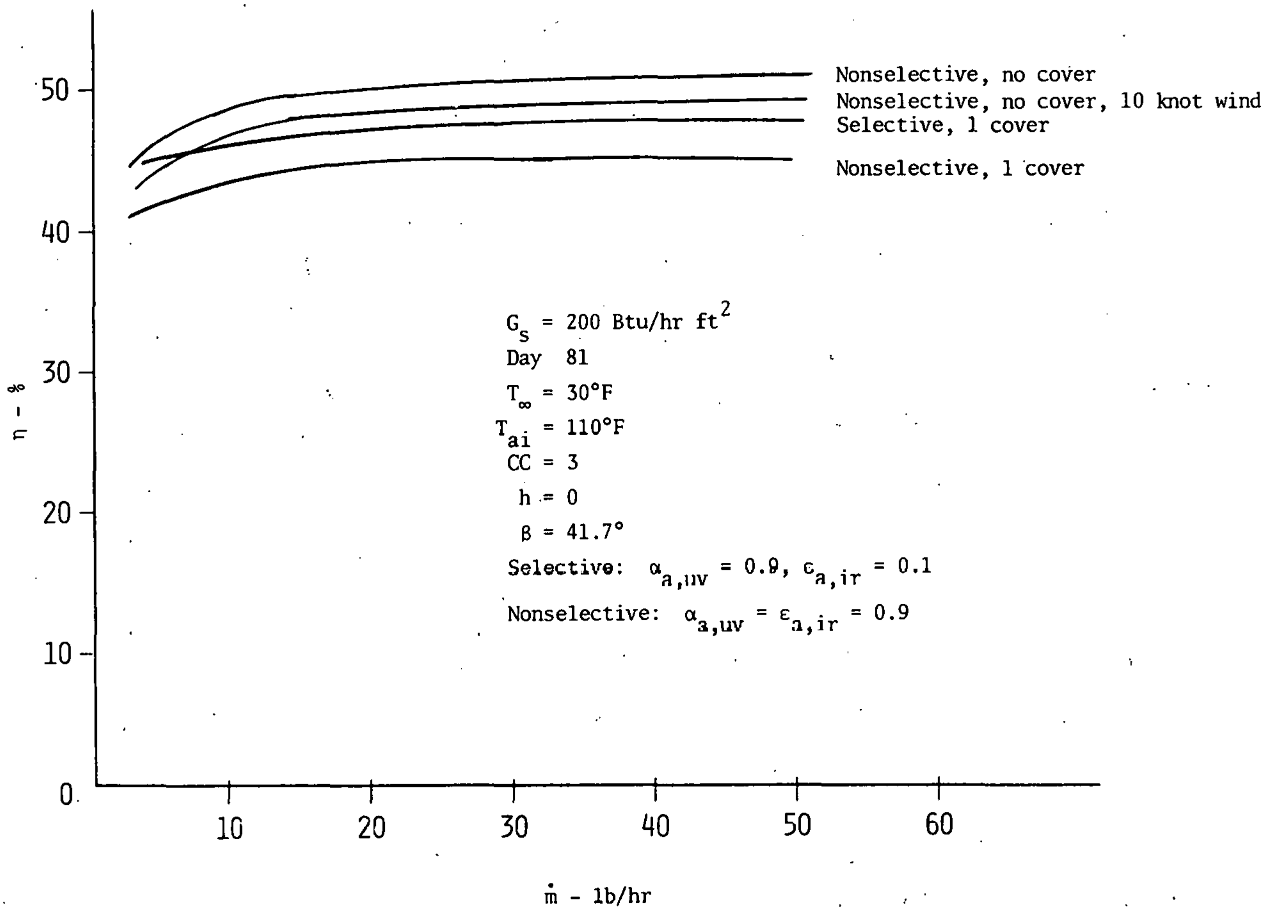

Fig. A.6. Midday Efficiency vs Flow Rate for CR = 10.

e. Effect of Selective Surface

Figs. A.4–A.6 show that a selective surface always improves performance. The selective surface used assumed surface properties of $\alpha_{a,uv}$ = 0.9 and $\varepsilon_{a,ir}$ = 0.1.

f. Other Effects

Wind speed and ambient-temperature effects are not great for a covered collector, except during extreme conditions. The effect of tilt is similar to that for other collectors, except that seasonal adjustments may be needed for larger CR collectors because of the CPC angular acceptance restriction. This property of the CPC has been treated thoroughly by Winston.[11]

The effect of time of day is shown in Fig. A.8. As the sun moves away from noon (in the Ptolemaic sense), the angle of incidence increases and cover reflection and absorption losses increase. These two synergistic effects cause a significant dropoff in efficiency with hour angle and are a fundamental source of reduced performance in a nontracking collector.

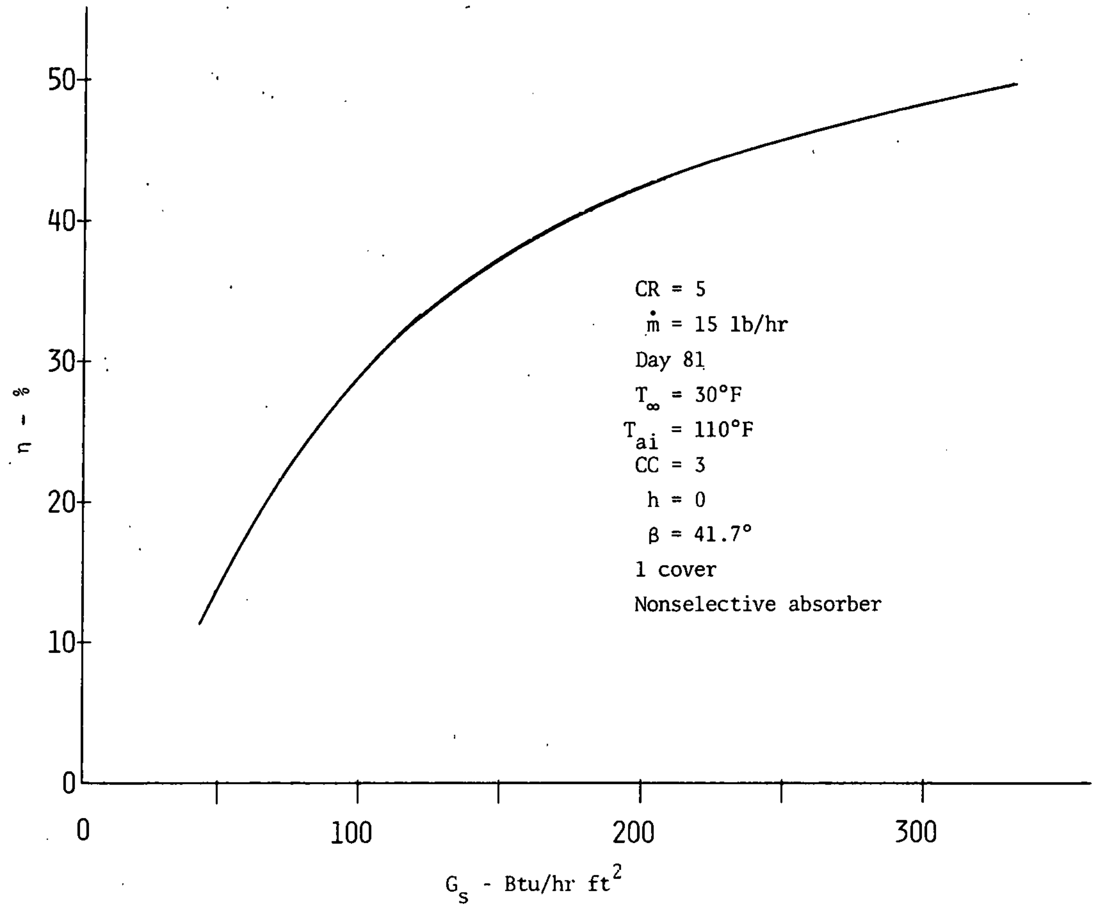

Fig. A.7. Midday Efficiency vs Direct Insolation.

The transmission portion of the loss can be eliminated by removing the cover, but this is done at the expense of increased convection losses.

Wet steam as a working fluid can have advantages, since the absorber temperature remains constant. If steam at subatmospheric pressure is used, improved performance over that of water at the same inlet temperature is experienced. Collector performance for three steam pressures is shown in Fig. A.9. Other parametric effects on a steam-cooled collector are similar to those described above for water.

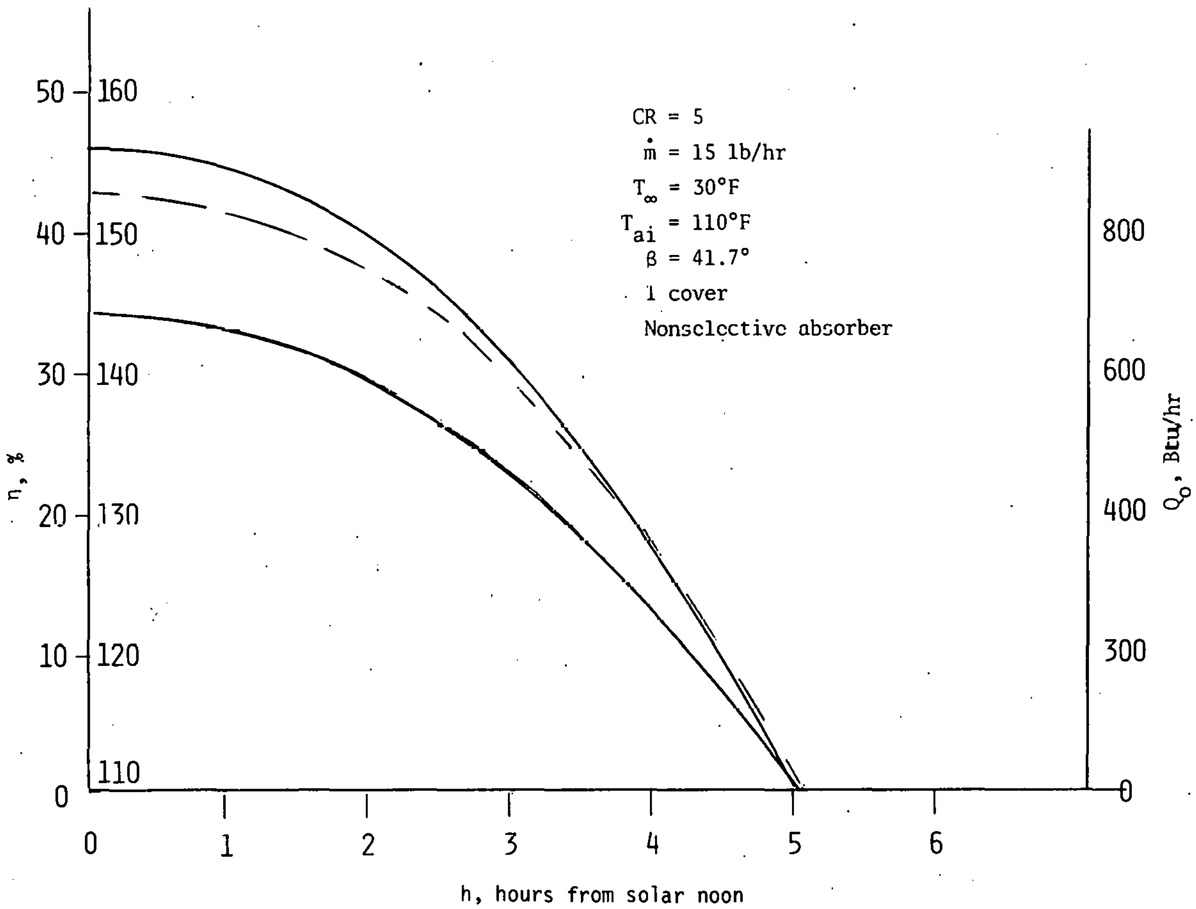

Fig. A.8. Hourly Performance for Day-81, Equinox.

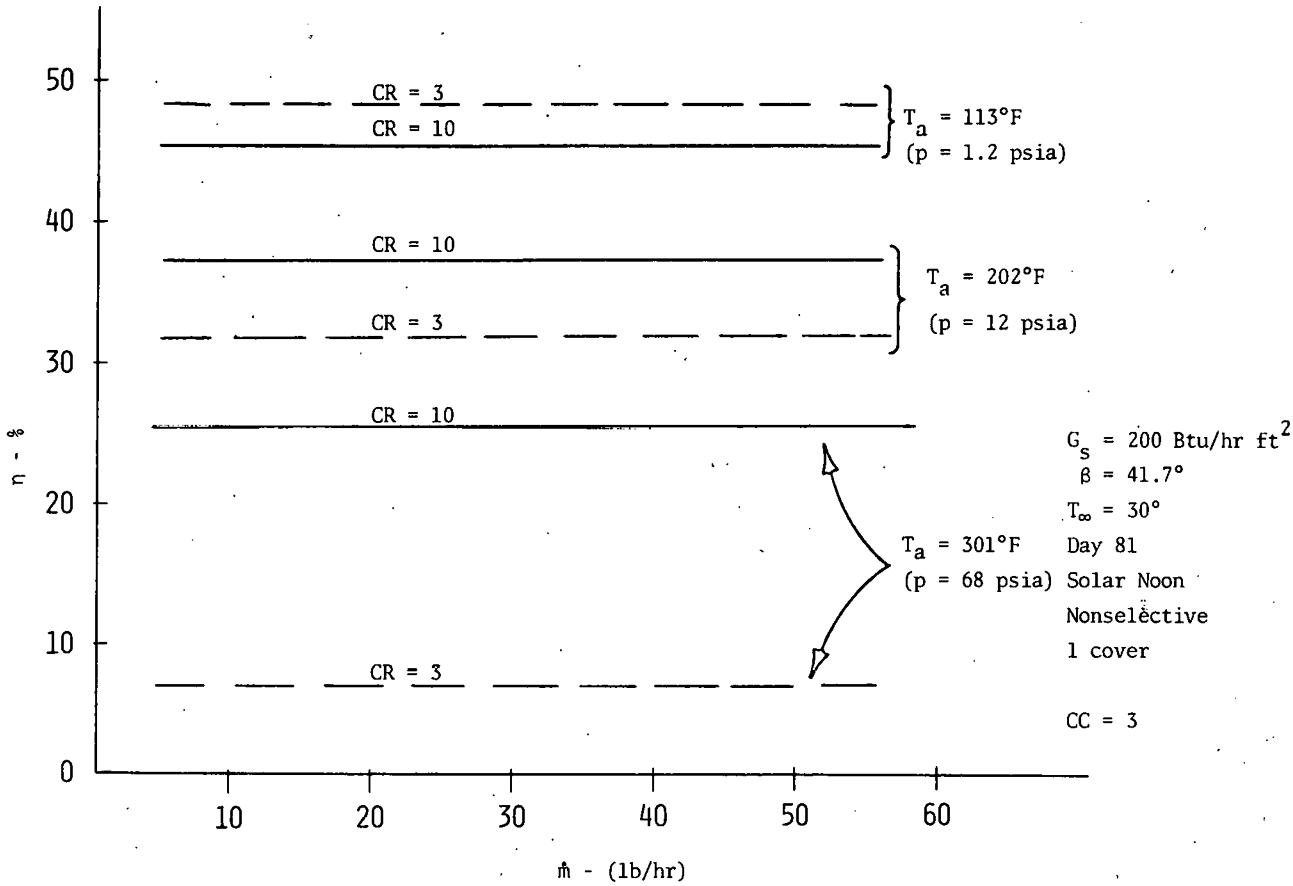

Fig. A.9. CPC Performance for Weat-steam Working Fluid.

g. Nomenclature*

Symbol	FORTRAN Symbol	Description	Units
C	C	Solar altitude angle projected on transverse plane	deg
CC	CC	Cloud cover (0, clear; 10, overcast)	-
-	CP	Specific heat of water	Btu lb^{-1} $^{o}R^{-1}$
CR	CR	Concentration ratio	-
DAY	DAY	Day number from January 1	-
Gr_L	GR	Grashof Number ($\rho^2 L^3 g \Delta T/\mu^2 T$)	-
G_s	GS	Direct insolation	Btu $hr^{-1} ft^{-2}$
h	H	Hour angle from noon, enthalpy	-, Btu lb^{-1}
$h_{c,ae}$	HCAE	Convective coefficient, absorber to cover	Btu $hr^{-1} ft^{-2}$ $^{o}R^{-1}$
$h_{c,e}$	HCE	Convective coefficient, cover to environment	Btu $hr^{-1} ft^{-2}$ $^{o}R^{-1}$
h_{coll}	XHCOLL, HCOLL	Collector height	in., ft
i	INC	Solar incidence angle	rad
-	K	Extinction coefficient of cover	$in.^{-1}$
L	XLAT, LAT	Collector latitude	deg, rad
L_C	LC	Collector length	ft
$\dot{m}$	XMDOT, MDOT	Fluid flow rate	lb hr^{-1}, lb $hr^{-1} ft^{-2}$
n_r	NR	Index of refraction of cover	-
P_r	PR	Prandtl Number ($C_p \mu/k$)	-
P_∞	XPINF, PINF	Ambient pressure	in.Hg, psia

*Infrequently used notation or notation used intermediately in CPCMOD calculations is not included.

Symbol	FORTRAN Symbol	Description	Units
$Q_{c,ae}$	QCAE	Convection exchange between cover and absorber	Btu $hr^{-1}ft^{-2}$
$Q_{c,e}$	QCE	Convection from cover to environment	Btu $hr^{-1}ft^{-2}$
$Q_{d,a}$	QDA	Diffuse solar radiation absorbed by absorber	Btu $hr^{-1}ft^{-2}$
$Q_{d,e}$	QDE	Diffuse solar radiation absorbed by cover	Btu $hr^{-1}ft^{-2}$
$Q_{e,sky}$	QESKY	Infrared radiation from cover to sky	Btu $hr^{-1}ft^{-2}$
$Q_{ir,ae}$	QIRAE	Infrared radiation exchange between cover and absorber	Btu $hr^{-1}ft^{-2}$
Q_o	QX	Useful energy delivered by collector	Btu $hr^{-1}ft^{-2}$
$Q_{uv,a}$	QUVA	Direct solar radiation absorbed by absorber	Btu $hr^{-1}ft^{-2}$
$Q_{uv,e}$	QUVE	Direct solar radiation absorbed by cover	Btu $hr^{-1}ft^{-2}$
r	REFL	Average number of reflections	-
Re_L	RE	Reynolds Number (VL/ν)	-
t_g	TG	Cover thickness	in.
T_a	TA(I)	Absorber temperature	^oR
T_{ai}	XTAIN, TAIN	Fluid inlet temperature	^oF, ^oR
T_{ao}	TAOUT	Fluid outlet temperature	^oR
T_e	TE(I)	Cover temperature	^oR
T_{sky}	TSKY	Sky temperature for radiation	^oR
T_∞	XTINF, TINF	Ambient temperature	^oF, ^oR
W_a	XWA, WA	Absorber width	in., ft
W_e	XWE, WE	Cover width	in., ft

Symbol Greek	FORTRAN Symbol	Description	Units
-	WIND	Average wind speed	knots
X_D	XD	Diffuse, skylight radiation	Btu $hr^{-1} ft^{-2}$
α	ALT	Solar altitude	deg
$\alpha_{a,d}$	AAD	Absorber diffuse solar (skylight) absorptance	-
$\alpha_{a,uv}$	AAUV	Absorber direct solar absorptance	-
$\alpha_{e,d}$	AED	Cover diffuse solar (sky light) absorptance	-
$\alpha_{e,uvd}$	AEUVD	Cover diffuse solar absorptance	-
$\alpha_{e,uv(i)}$	AEUV	Cover direct solar absorptance	-
β	XBETA, BETA	Collector tilt	deg, rad
δ_s	DEC	Solar declination	rad
$\varepsilon_{a,ir}$	EAIR	Absorber IR emittance	-
ε_{eff}	EEFF	Effective IR emittance, cover to absorber	-
$\varepsilon_{e,ir}$	EEIR	Cover IR emittance	-
η	EFF	Efficiency	-
$\rho_{a,uv}$	RAUV	Absorber direct solar reflectance	-
$\rho_{e,ir}$	REIR	Cover IR reflectance	-
$\rho_{e,uv(i)}$	REUV	Cover direct solar reflectance	-
$\rho_{e,uvd}$	REUVD	Cover diffuse solar reflectance	-
ρ_m	RM	Mirrored surface reflectance	-
σ	SIGMA	Stefan-Bottzmann constant	Btu $hr^{-1} ft^{-2} {}^oR^{-1}$
$\tau_{e,d}$	TED	Cover diffuse solar (skylight) transmittance	-

Symbol Greek	FORTRAN Symbol	Description	Units
$\tau_{e,uv(i)}$	TEUV	Cover direct solar transmittance	–

7. Listing of CPCMOD Program

```
      PROGRAM CPCMOD(INPUT,OUTPUT)
C**THIS PROGRAM COMPUTES THE PERFORMANCE OF THE COMPOUND PARABOLIC
C   SOLAR COLLECTOR UNDER DEVELOPMENT AT ARGONNE NATIONAL LABORATORY
C   PROGRAM VERSION SEPTEMBER 15, 1974 WRITTEN BY JK
C   COMPUTATIONS ARE CARRIED OUT FOR ONE HALF OF EACH DAY SPECIFIED.
C   PERFORMANCE IS COMPUTED AT TIME INTERVALS SELECTED BY THE USER (DDT)
C   MODEL WILL MAKE REPEATED RUNS IN WHICH ONE PARAMETER IS VARIED THRU
C   A RANGE OF VALUES.  ALL OTHER PARAMETERS WILL REMAIN THE SAME.
C   MODEL RUN EXECUTION IS ACTIVATED BY A 9 IN COL 1 OF A DATA CARD
C   PROGRAM RUN IS TERMINATED BY THE WORD STOP IN COL 1-4 OF LAST CARD
      DIMENSION TITLE(8),TA(2),GM(3),TE(2)
      DIMENSION XX(8)
      REAL MDOT,LC,LAT,NR,NDAY,K,INC
      FDEC(T)=(-23.5*3.14159/180.)*COS(6.28318*(T+10.5)/365.)
      FTSKY(X)=0.914*X
      FINC(D,XL,B,H)=SIN(D)*SIN(XL-B)+COS(D)*COS(XL-B)*COS(H)
      FALT(D,XL,H)=SIN(D)*SIN(XL)+COS(D)*COS(XL)*COS(H)
      DATA (GM(I),I=1,3)/19.,11.,5./
      SIGMA=.1714E-8
      PI=4.*ATAN(1.0)
      CP=1.
969   READ 1,(TITLE(I),I=1,8)
1     FORMAT(A5,7A10)
      IF(TITLE(1).EQ.5HSTOP )CALL EXIT
      IF(TITLE(1).EQ.5HSTEAM)IFSTM=1
      IF(TITLE(1).NE.5HSTEAM)IFSTM=0
101   READ 2,(IT,(XX(I),I=1,7))
2     FORMAT(I1,7F10.0)
      GO TO (11,12,13,14,15,16,17,18,19)IT
C**READ IN METEOROLOGICAL DATA
11    GS=XX(1)
      WIND=XX(2)

      XTINF=XX(3)
      XPINF=XX(4)
      DAY=XX(5)
      XLAT=XX(6)
      CC=XX(7)
      PINF=XPINF*14.696/30.
      TINF=XTINF+459.7
      LAT=XLAT*PI/180.
      GSSTOR=GS
      GO TO 101
C**READ IN ABSORBER RADIATION PROPERTIES
12    AAUV=XX(1)
      EAIR=XX(2)
      AAD=XX(3)
      RAUV=1.-AAUV
      RAIR=1.-EAIR
      GO TO 101
C**READ IN COVER RADIATION PROPERTIES
13    REUVD=XX(1)
      AEUVD=XX(2)
      TG=XX(3)
      NR=XX(4)
```

```
      K=XX(5)
      TED=XX(6)
      AED=XX(7)
      IF(TG.EQ.0.)IC=0
      IF(TG.NE.0.)IC=1
      GO TO 101
14    EEIR=XX(1)
      REIR=XX(2)
      GO TO 101
C**READ IN COLLECTOR PARAMETERS
15    LC=XX(1)
      XHCOLL=XX(2)
      RM=XX(3)
      CR=XX(4)
      XWE=XX(5)
      XWA=XX(6)
      XBETA=XX(7)
      WE=XWE/12.
      WA=XWA/12.
      HCOLL=XHCOLL/12.
      AA=LC*WA
      AE=LC*WE
      IF(CR.EQ.3.)ICR=1
      IF(CR.EQ.5.)ICR=2
      IF(CR.EQ.10.)ICR=3
      BETA=XBETA*PI/180.
      GO TO 101
C**READ IN COLLECTOR OPERATING CONDITION AND COMPUTATIONAL PARAMETERS
16    XMDOT=XX(1)
      XTAIN=XX(2)
      DDT=XX(3)
      FN=12./DDT
      N=FN
      NHP1=N+1
      TAIN=XTAIN+459.7
      GO TO 101
17    CONTINUE
18    CONTINUE
19    CONTINUE

C**PRINT OUT ALL INPUT DATA
      PRINT 20,(TITLE(I),I=1,8)
20    FORMAT(1H1,A5,7A10//)
      PRINT 21,GSSTOR,WIND,XTINF,XPINF,DAY,XLAT,CC
21    FORMAT(1H0*CLIMATOLOGICAL DATA:*/
     15X* DIRECT INSOLATION (BTU/HRSQFT):*4X,F5.0/
     25X* AVERAGE WIND SPEED (KNOTS):*10X,F3.0/
     35X* AMBIENT TEMPERATURE (DEG F):*8X,F4.0/
     45X* AMBIENT PRESSURE (IN HG):*11X,F4.0/
     55X* DAY OF YEAR FROM JAN 1:*13X,F4.0/
     65X* LATITUDE OF COLLECTOR (DEG):*8X,F4.1/
     75X* AVERAGE CLOUD COVER INDEX:*12X,F2.0/)
      PRINT 22,AAUV,EAIR,AAD
22    FORMAT(1H0*ABSORBER RADIATION PROPERTIES:*/
     15X* ABSORBER UV ABSORPTANCE:*12X,F4.2/
     25X* ABSORBER IR EMITTANCE:*14X,F4.2/
```

```
     35X* ABSORBER SKYLIGHT ABSORPTANCE:*6X,F4.2/)
      PRINT 23,REUVD,AEUVD,TG,NR,K,TED,AED,EEIR,REIR
23    FORMAT(1H0*COLLECTOR COVER PROPERTIES:*/
     25X* COVER DIFFUSE UV REFLECTANCE:*7X,F4.2/
     25X* COVER DIFFUSE UV ABSORPTANCE:*7X,F4.2/
     35X* COVER MATERIAL THICKNESS (IN):*5X,F5.3/
     45X* COVER REFRACTIVE INDEX:*12X,F5.3/
     55X* COVER EXTINCTION COEFFICIENT(/IN):*2X,F4.3/
     65X* COVER SKYLIGHT TRANSMITTANCE:*7X,F4.2/
     75X* COVER SKYLIGHT ABSORPTANCE:*9X,F4.2/
     85X* COVER IR EMITTANCE:*17X,F4.2/
     95X* COVER IR REFLECTANCE:*15X,F4.2/)
      PRINT 24,LC,XHCOLL,RM,CR,XWE,XWA,XBETA
24    FORMAT(1H0*COLLECTOR SPECIFICATIONS:*/
     15X* COLLECTOR LENGTH (FT):*13X,F5.2/
     25X* COLLECTOR HEIGHT (IN):*13X,F5.2/
     35X* COLLECTOR REFLECTANCE:*14X,F4.2/
     45X* NOMINAL CONCENTRATION RATIO:*9X,F3.0/
     55X* APERTURE WIDTH (IN):* 15X,F5.2/
     65X* ABSORBER WIDTH (IN):*15X,F5.2/
     75X* COLLECTOR TILT (DEG):*15X,F4.1/)
      PRINT 25,XMDOT,XTAIN,DDT
25    FORMAT(1H0*OPERATING AND COMPUTATIONAL PARAMETERS:*/
     15X* FLOW RATE (LB/HR):*12X,F10.2/
     25X* FLUID INLET TEMPERATURE:*12X,F4.0/
     35X* TIME INCREMENT (HR):*16X,F4.1)
C**CALCULATE ANGLES FOR HALF DAY ITERATION
      TSKY=FTSKY(TINF)
      DEC=FDEC(DAY)
      HS=ABS(ACOS(-TAN(LAT)*TAN(DEC)))
C**CALCULATE RADIATION VIEW FACTORS
      IF(IC.EQ.0)GO TO 27
      CALL SHAPE(LC,WE,WA,HCOLL,F1245)
      FAM=1.-F1245
      FEM=1.-WA*F1245/WE
      EEF=1./((RAIR/EAIR)+((REIR/EEIR)*(WA/WE))+
     1(1./(F1245+1./((1./FAM)+(WA/WE*FEM)))))
27    TA(1)=TAIN
      TE(1)=TINF
      MDOT=XMDOT/(LC*WA)

      DO 999 I=1,NHP1
      FI=I
      H=(FI-1.)*DDT*15.*PI/180.
      IF(H.GT.HS)GO TO 80
      COSINC=FINC(DEC,LAT,BETA,H)
      IF (COSINC.LT.0.)GO TO 77
      INC=ACOS(COSINC)
C**COMPUTE SOLAR INCIDENCE ANGLE IN THE COLLECTOR TRANSVERSE PLANE
      SINALT=FALT(DEC,LAT,H)
      ALT=ABS(ASIN(SINALT))
      XALT=ALT*180./PI
      C=ATAN((SIN(ALT)*COS(LAT))/(SIN(ALT)*SIN(LAT)-SIN(DEC)))*180./PI
      GAMMA=ABS(90.-XBETA-C)
      IF(GAMMA.GT.GM(ICR))GS=0.
      IF(GAMMA.LE.GM(ICR))GS=GSSTOR
```

```
C**COMPUTE COVER RADIATION PROPERTIES FROM STOKES EQUATIONS
      SINREF=SIN(INC)/NR
      AREF=ASIN(SINREF)
      PATH=TG/COS(AREF)
      GG=EXP(-K*PATH)
      IF(INC.EQ.0.)RHOG=((NR-1.)/(NR+1.))**2.
      IF(INC.NE.0.)
     1RHOG=0.5*(((SIN(INC-AREF)*SIN(INC-AREF))/
     2(SIN(INC+AREF)*SIN(INC+AREF)))+
     3(TAN(INC-AREF)*TAN(INC-AREF))/
     4(TAN(INC+AREF)*TAN(INC+AREF)))
      REUV=RHOG+(1.-RHOG)*(1.-RHOG)*RHOG*GG*GG/(1.-RHOG*RHOG*GG*GG)
      TEUV=(1.-RHOG)*(1.-RHOG)*GG/((1.-RHOG*GG)*(1.+RHOG*GG))
      AEUV=1.-REUV-TEUV
C**CALCULATE HEAT FLUX TERMS
      QUVA=GS*(RM**REFL(GAMMA,CR))*COSINC*TEUV*AAUV*(1.+
     1RAUV*REUVD)*WE/WA
      QUVE=GS*COSINC*(AEUV+TEUV*(RM**REFL(GAMMA,CR))*RAUV*AEUVD)*WE/WA
      XD=0.78+1.07*XALT+6.17*CC
      QDA=XD*TED*AAD
      QDE=XD*AED*WE/WA
903   CONTINUE
      QIRAE=EEF*SIGMA*(TA(1)**4.-TE(1)**4.)
      IF(IC.EQ.0)QIRAE=EAIR*SIGMA*(TA(1)**4.-TSKY**4.)
      QCAE=HCAE(TA(1),TE(1),PINF,WE,WA,BETA)*(TA(1)-TE(1))
      IF(IC.EQ.0)QCAE=HCE(WIND,TA(1),TINF,PINF,LC,BETA,WE)*(TA(1)-TE(1))
      QESKY=EEIR*SIGMA*(TE(1)**4.-TSKY**4.)*WE/WA
      IF(IC.EQ.0)QESKY=0.
      QCE=HCE(WIND,TE(1),TINF,PINF,LC,BETA,WE)*(TE(1)-TINF)*WE/WA
      IF(IC.EQ.0)QCE=0.
      IF(IC.EQ.0)GO TO 67
C**SOLVE FOR TE ITERATIVELY BY NEWTONS METHOD
      FTE=QESKY+QCE-QUVE-QIRAE-QCAE-QDE
      FPTE=(4.*WE*EEIR*SIGMA*TE(1)**3.)/WA+
     1HCE(WIND,TE(1),TINF,PINF,LC,BETA,WE)*WE/WA
     2+4.*EEFF*SIGMA*TE(1)**3.+HCAE(TA(1),TE(1),PINF,WE,WA,BETA)
      TE(2)=TE(1)-FTE/FPTE
      IF(TE(2).LT.0.)TE(2)=0.
      DT=ABS(TE(1)-TE(2))
      IF(DT.GT.0.1)TE(1)=TE(2)
      IF(DT.GT.0.1)GO TO 903
67    QX=QUVA-QIRAE-QCAE+QDA
      TAOUT=QX/(MDOT*CP)+TAIN
      IF(IFSTM.EQ.1)TAOUT=TAIN
C**ITERATE FOR VALUE OF TA IF REQUIRED
      TA(2)=(TAOUT+TAIN)/2.
      DT=ABS(TA(2)-TA(1))
      IF(DT.GT.0.1)TA(1)=TA(2)
      IF(DT.GT.0.1)GO TO 903
      HOUR=(FI-1.)*DDT
      XTE=TE(1)-459.7
      XTAOUT=TAOUT-459.7
      QOUT=QX*AA
C**COMPUTE COLLECTION EFFICIENCY BASED UPON TOTAL INCIDENT RADIATION
      EFF=QOUT/((GSSTOR+XD)*AE)*100.
      IF(H.EQ.0.)PRINT 71
```

```
71    FORMAT(1H1*PERFORMANCE RESULTS*//
     11X*HOUR*2X*COLLECTION*2X*EFFICIENCY*2X*INLET TEMP*
     22X*OUTLET TEMP*2X*COVER TEMP*//)
      PRINT 72,HOUR,QOUT,EFF,XTAIN,XTAOUT,XTE
72    FORMAT(2X,F3.1,5X,F7.0,7X,F5.1,6X,F6.1,7X,F6.1,6X,F6.1/)
999   CONTINUE
      GO TO 969
77    PRINT 78
78    FORMAT(1H0*COLLECTION PERIOD TERMINATED - INCIDENCE ANGLE GREATER
     1THAN 90 DEGREES*)
      GO TO 969
80    PRINT 81
81    FORMAT(1H0*COLLECTION PERIOD TERMINATED - SUNSET*)
      GO TO 969
      END
```

```
      SUBROUTINE SHAPE(XLC,WE,WA,HCOLL,F1245)
C**THIS SUBROUTINE CALCULATES THE RADIATION SHAPE FACTORS
      REAL LC
      F12(X,Y)=(2./(3.14159265*X*Y))*(ALOG(SQRT((1.+X*X)*(1.+Y*Y)/(1.+
     1X*X+Y*Y)))+Y*SQRT(1.+X*X)*ATAN(Y/(SQRT(1.+X*X)))+
     2X*SQRT(1.+Y*Y)*ATAN(X/(SQRT(1.+Y*Y)))-
     2Y*ATAN(Y)-X*ATAN(X))
      LC=XLC
      A1=LC*WA
      A3=0.5*(WE-WA)*LC
      A13=A1+A3
C**SHAPE FACTOR F1324
      X1=LC/HCOLL
      Y1=0.5*(WA+WE)/HCOLL
      F1324=F12(X1,Y1)
C**SHAPE FACTOR F34
      X2=LC/HCOLL
      Y2=0.5*(WE-WA)/HCOLL
      F34=F12(X2,Y2)
      F1245=(1./A1)*(A13*F1324-A3*F34)
      RETURN
      END
```

```
C**THIS SUBROUTINE DETERMINES THE REFLECTANCE EXPONENT TO BE APPLIED TO
C  THE MIRROR SURFACE REFLECTANCE
```

```
      FUNCTION REFL(X,CR)
      IF(CR.EQ.5.)GO TO 5
      IF(CR.EQ.10.)GO TO 10
      IF(X.LT.1.90.AND.X.GE.0.00)REFL=0.80
      IF(X.LT.2.85.AND.X.GE.1.90)REFL=0.81
      IF(X.LT.3.80.AND.X.GE.2.85)REFL=.78
      IF(X.LT.4.75.AND.X.GE.3.80)REFL=.76
      IF(X.LT.5.70.AND.X.GE.4.75)REFL=.73
      IF(X.LT.6.65.AND.X.GE.5.70)REFL=.70
      IF(X.LT.7.60.AND.X.GE.6.65)REFL=.68
      IF(X.LT.8.55.AND.X.GE.7.60)REFL=.67
      IF(X.LT.9.50.AND.X.GE.8.55)REFL=.66
      IF(X.LT.15.20.AND.X.GE.9.50)REFL=.69
      IF(X.LT.16.15.AND.X.GE.15.20)REFL=.71
      IF(X.LT.17.10.AND.X.GE.16.15)REFL=.73
      IF(X.LT.19.00.AND.X.GE.17.10)REFL=.77
      RETURN
5     IF(X.LT.0.55.AND.X.GE.0.00)REFL=1.11
      IF(X.LT.1.65.AND.X.GE.0.55)REFL=1.09
      IF(X.LT.2.20.AND.X.GE.1.65)REFL=1.05
      IF(X.LT.2.75.AND.X.GE.2.20)REFL=1.04
      IF(X.LT.3.30.AND.X.GE.2.75)REFL=1.02
      IF(X.LT.3.85.AND.X.GE.3.30)REFL=1.00
      IF(X.LT.4.40.AND.X.GE.3.85)REFL=0.95
      IF(X.LT.4.95.AND.X.GE.4.40)REFL=0.90
      IF(X.LT.5.50.AND.X.GE.4.95)REFL=0.85
      IF(X.LT.6.05.AND.X.GE.5.50)REFL=0.83
      IF(X.LT.11.0.AND.X.GE.6.05)REFL=0.80
      RETURN
10    IF(X.LT.1.75.AND.X.GE.0.00)REFL=1.29
      IF(X.LT.2.00.AND.X.GE.1.75)REFL=1.26
      IF(X.LT.2.25.AND.X.GE.2.00)REFL=1.23
      IF(X.LT.2.50.AND.X.GE.2.25)REFL=1.20
      IF(X.LT.2.75.AND.X.GE.2.50)REFL=1.16
      IF(X.LT.3.00.AND.X.GE.2.75)REFL=1.12
      IF(X.LT.3.25.AND.X.GE.3.00)REFL=1.08
      IF(X.LT.3.50.AND.X.GE.3.25)REFL=1.07
      IF(X.LT.3.75.AND.X.GE.3.50)REFL=1.04
      IF(X.LT.4.00.AND.X.GE.3.75)REFL=1.01
      IF(X.LT.4.25.AND.X.GE.4.00)REFL=0.99
      IF(X.LT.4.50.AND.X.GE.4.25)REFL=0.97
      IF(X.LT.4.75.AND.X.GE.4.50)REFL=0.93
      IF(X.LT.5.00.AND.X.GE.4.75)REFL=0.93
      RETURN
      END
```

```
      FUNCTION HCAE(TE,TA,PINF,WE,WA,BETA)
C**THIS SUBROUTINE DETERMINES THE COEFFICIENT OF CONVECTIVE HEAT
C  TRANSFER BETWEEN THE ABSORBER AND THE COVER (IF ANY)
      REAL KK,NU
      G=32.17
      PR=.7
      RA=53.3
      TM=0.5*(TE+TA)
      VIS=1.7*(TM**0.67)/10000000.
      KK=0.343*3600.*VIS
      RHO=PINF*144./(RA*TM)
      GR=RHO*RHO*G*COS(BETA)*WA*WA*WA*ABS(TA-TE)/(VIS*VIS*TM)
      NU=0.54*(GR*PR)**.25
      HC=KK*NU/WA
      HCAE=1./((1./HC)+(WA/(WE*HC)))
      RETURN
      END
```

```
      FUNCTION HCE(WIND,TE,TINF,PINF,LC,BETA,WE)
C**THIS SUBROUTINE DETERMINES THE COEFFICIENT OF FORCED OR FREE CON-
C  VECTION BETWEEN THE COLLECTOR COVER AND THE ENVIRONMENT
C  IF THE WIND SPEED IS LESS THAN 0.5 KT, FREE CONVECTION DOMINATES
      REAL KK,NUEX,LC
      G=32.17
      PR=.7
      RA=53.3
      TM=0.5*(TE+TINF)
      VIS=1.7*(TM**0.67)/10000000.
      KK=0.343*3600.*VIS
      RHOFILM=PINF*144./(RA*TM)
      IF(WIND.GE.0.5)GO TO 10
C**FREE CONVECTION
      GREX=RHOFILM*RHOFILM*G*SIN(BETA)*WE*WE*WE*ABS(TE-TINF)/(VIS*VIS*TM
     1)
      IF(GREX.GT.700000000.)NUEX=0.10*(GREX*PR)**.333
      NUEX=0.555*(GREX*PR)**.25
      HCE=KK*NUEX/WE
      RETURN
C**FORCED CONVECTION
C  WIND HAS UNITS OF KNOTS PER NWS
10    RE=WIND*1.13*1.46*LC*RHOFILM/VIS
      IF(RE.LT.500000.)NUEX=0.664*SQRT(RE)*PR**.333
      IF(RE.GE.500000.)NUEX=0.036*(PR**.333)*(RE**.8-23200.)
      HCE=KK*NUEX/LC
      RETURN
      END
```

8. Summary--Performance Study of the Compound Parabolic Concentrator Solar Collector

We have studied the heat-transfer characteristics of CPC's coupled with a thermal-heat-exchange system using a computer simulation devised by Dr. Jan Kreider of Environmental Consultants, Boulder, Colorado. Using data on the optical properties of the CPC supplied by us, Dr. Kreider's program includes all first-order radiative and conductive heat-transfer mechanisms. The program models a single trough and neglects the heat loss through the sides and back of the collector, since, in practice, one may minimize these losses with sufficient insulation.

Dr. Kreider's program needed some modification to be able to run on the IBM 370 available at the University. These modifications were due to some dissimilar FORTRAN conventions and involved extensive format changes and a careful checking of formulas to ensure accurate computer representation. Runs were then made to ensure the credibility of the program.

During testing of the X3 and X10 concentrators at Argonne National Laboratory, we matched the program parameters as closely as possible to the test situation. The results of the program have improved our understanding of the heat-transfer processes in the collector.

For the purpose of evaluating collector configurations, we singled out a parameter that can be easily measured on our experimental arrangement and that can be calculated from the computer results. The efficiency of a collector as a function of temperature is of the form

$$\eta(T) = \eta(T_{amb}) - \frac{U_L(T - T_{amb})}{S} ,$$

where T_{amb} is the ambient temperature and S is the solar flux. For our collectors and over a wide range of temperatures, U_L is approximately independent of temperature. This factor represents the slope of an efficiency; versus operating-temperature curve as shown in Figs. A.10 and A.11.

Figs. A.10 and A.11 are graphs of performance results for an X3 and X10 concentrator taken from the results of a simulation program. For the X3 concentrator, the heat losses are approximately linear with $\Delta T/S$, and we obtain a value for $U_L \simeq 0.60$. The temperature range spanned here is from ambient to 250°F. For the X10 collector, the linear approximation is no longer quite true, but the temperature range considered here is from ambient to 500°F. If we consider the temperature range of the X10 test unit, we get a $U_L \simeq 0.22$.

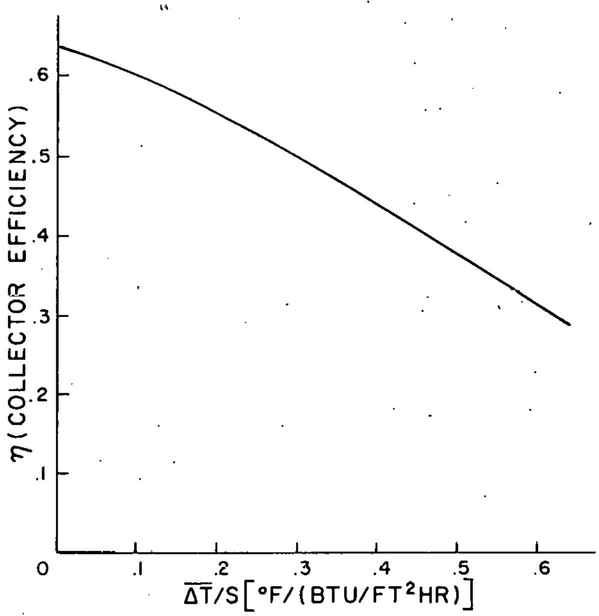

Fig. A.10. Computer Simulation of X3 Collector. Flow rate, 5 lb hr^{-1}. No clouds, one cover. Wind speed, 10 knots.

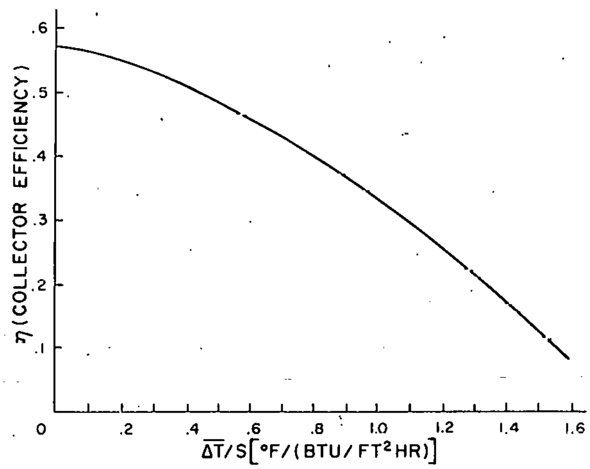

Fig. A.11. Computer Simulation of X10 Collector. No clouds, one cover. Wind speed, 10 knots.

APPENDIX B

PRINCIPLES OF CYLINDRICAL CONCENTRATORS FOR SOLAR ENERGY

R. Winston and H. Hinterberger*

ABSTRACT

Ideal cylindrical light collectors are trough-like reflecting-wall light channels of a specific shape which concentrate radiant energy by the maximum amount allowed by phase-space conservation. We propose a principle for maximally concentrating radiation onto a tube receiver of general shape. Using this principle, we give a general prescription for designing concentrators appropriate to such tube receivers. This design may have advantages for solar-thermal and photovoltaic applications.

1. Introduction

In a recent paper, a cylindrical mirror was proposed for concentrating radiant energy by the maximum amount permitted by physical principles (phase-space conservation).[1] This mirror collects radiation over an entrance aperture of width d_1, and an angular field of view of θ_{max} (half angle) in the plane transverse to the cylinder, and concentrates it onto an exit aperture of width d_2, where

$$d_1/d_2 = 1/\sin\theta_{max}. \tag{B.1}$$

The plane profile curve of this mirror as proposed by us in an earlier paper[5] consists of two distinct parabolas whose axes are inclined at angles $\pm\,\theta_{max}$ with respect to the optic axis of the collector; it should not be confused with the simple parabolic collector.

Here we propose a cylindrical mirror for concentrating radiation onto a tube of very general cross section. This cross section may, for example, be circular, oval, rectangular, or even fin-like. The concentration achieved is

$$d_1/S = 1/\sin\theta_{max}, \tag{B.2}$$

where S is the circumference of the tube. This design may have advantages over the compound parabolic one proposed in Ref. 1 for certain types of receivers, both solar-thermal and photovoltaic.

2. Principles of Concentrators

To motivate the present design, it is helpful to discuss the compound parabolic design from a different point of view.

Fig. B.1 is the transverse cross section of the cylindrical mirror. The origin is placed at the edge of the exit aperture. The extreme accepted

*Fermi National Accelerator Laboratory, Batavia, Illinois 60510

ray (direction cosines) is denoted by

$$\vec{k} = (\sin\theta_{max}, 0, -\cos\theta_{max}). \quad \text{(B.3)}$$

The dashed (shadow) lines intersect the edges of the exit aperture and are inclined at angle θ_{max} to the optic axis. The profile curve of the mirror $r(\phi)$ reflects the extreme ray into the origin. Thus,

$$dr/d\phi = -(d\vec{r}/d\phi) \cdot \vec{k}, \quad \text{(B.4)}$$

where the angle ϕ parameterizes the profile curve. We extend the curve $\vec{r}(\phi)$ to where it turns parallel to the optic axis and intersects the shadow lines. Then, integrating Eq. B.4, we obtain

$$r_1 - r_2 = -(\vec{r}_1 - \vec{r}_2) \cdot \vec{k}. \quad \text{(B.5)}$$

From the geometry of Fig. B.1,

$$r_1 = d_1 \sin\theta_{max} = (\vec{r}_1 - \vec{r}_2) \cdot \vec{k}. \quad \text{(B.6)}$$

Therefore,

$$r_2 = d_2 \quad \text{(B.7)}$$

and

$$d_2 = d_1 \sin\theta_{max}, \quad \text{(B.8)}$$

which agrees with Eq. B.1.

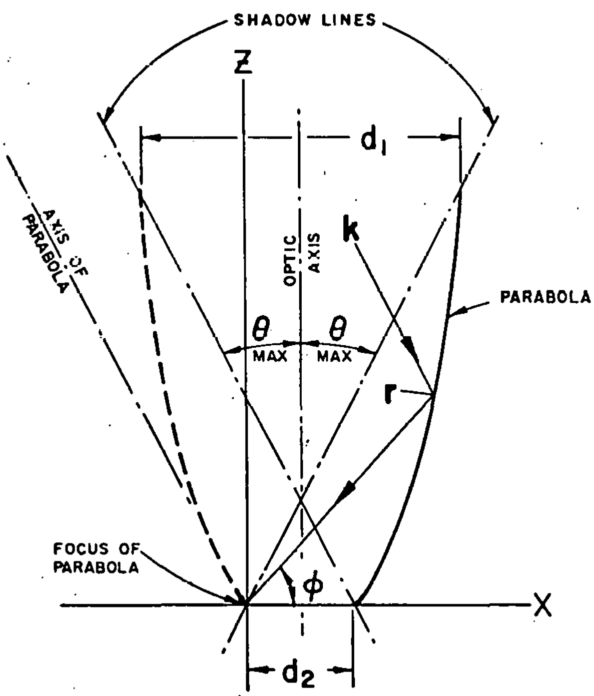

Fig. B.1. Profile Curve of the Compound Parabolic Concentrator. The axis of the parabola is inclined at angle θ_{max} to the optic axis.

Notice that we have obtained the concentration factor of Eq. B.1 without explicit reference to the parabolic form of the curve. It arises from integrating the condition imposed on the extreme ray in Eq. B.4, reminiscent of the way one obtains conservation laws. We remark that, with the extreme ray conditions satisfied, rays incident at angles $\theta > \theta_{max}$ are reflected out. It follows from phase-space conservation that all rays with angles $\theta < \theta_{max}$ are accepted.[3]

We may now proceed to the present design of a cylindrical mirror that maximally concentrates radiation onto the surface of a tube receiver. The tube's cross section may have any shape, provided only that it is convex and symmetric about the optic axis. In fact, the "tube's" surface need not even be closed. The convex requirement keeps a tangent from crossing the receiver boundary. With reference to Fig. B.2, the construction proceeds as follows:

To facilitate the discussion, we define some reference lines and points. The dashed (shadow) lines are tangent to the receiver at B and C and inclined at angle θ_{max} to the optic axis. Vectors $\vec{r}$ and $\vec{R}$ lie on the mirror and receiver, respectively. Both are parameterized by the arc length S along the circumference of the tube as measured from point A. It is convenient to write

$$\vec{r} = \vec{R} = \ell \vec{t} \qquad (B.9)$$

where

$$\vec{t} = d\vec{R}/dS \qquad (B.10)$$

is the tangent to the receiver and ℓ is the distance from R to r. Between points A and B, we impose

$$d\vec{r}/dS \cdot \vec{t} = 0, \qquad (B.11)$$

which is the usual condition for an involute. Then, since, from Eq. 9,

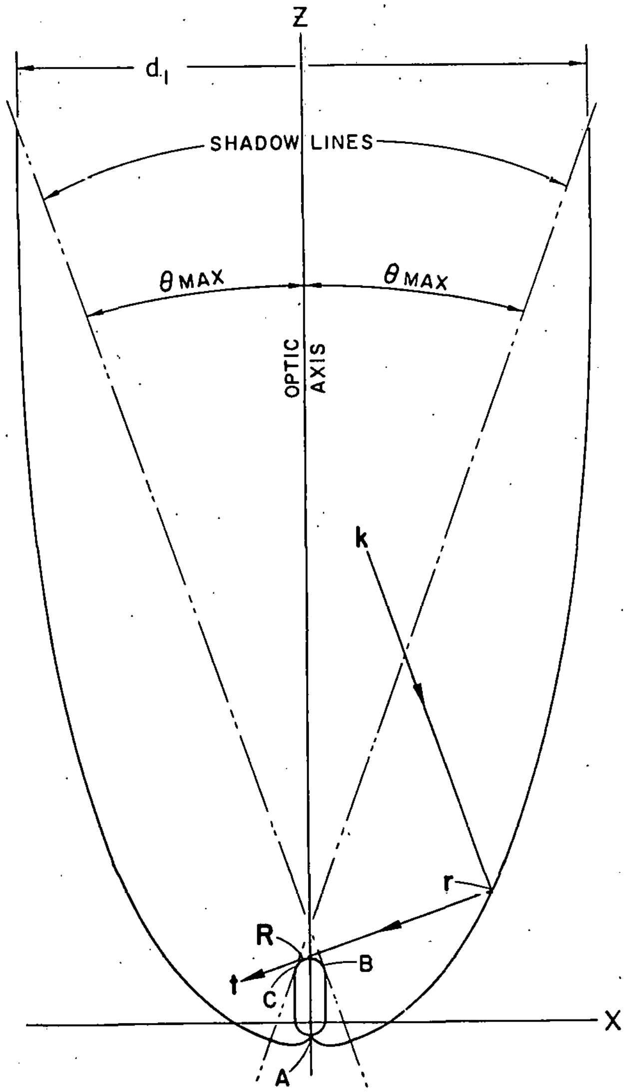

Fig. B.2. Profile Curve of X3 Concentrator for Oval Tube Receiver.

$$(d\underset{\rightarrow}{r}/dS) \cdot \underset{\rightarrow}{t} = 1 - d\ell/dS, \tag{B.12}$$

we obtain, upon integrating Eq. B.11 between points A and B,

$$S_B = \ell_B, \tag{B.13}$$

a familiar geometric property of the involute. Between points B and C, we require the extreme ray k to be reflected into the tangent $\underset{\rightarrow}{t}$ to the receiver in analogy with Eq. B.4. Thus,

$$(d\underset{\rightarrow}{r}/dS) \cdot \underset{\rightarrow}{t} = (d\underset{\rightarrow}{r}/dS) \cdot \underset{\rightarrow}{k}. \tag{B.14}$$

Since Eq. B.11 and B.14 coincide at point B, there is no discontinuity in slope.

Integrating Eq. B.14 between points B and C (using Eq. B.12 and B.13), we obtain

$$(S_C - S_B) - (\ell_C - \ell_B) = S_C - \ell_C = (\underset{\rightarrow}{r}_C - \underset{\rightarrow}{r}_B) \cdot \underset{\rightarrow}{k}. \tag{B.15}$$

From the geometry of Fig. B.2,

$$\ell_C + \ell_B = d_1 \sin\theta_{max} - (\underset{\rightarrow}{r}_C - \underset{\rightarrow}{r}_B) \cdot \underset{\rightarrow}{k}. \tag{B.16}$$

Therefore, we find for the circumference (using Eq. B.13),

$$S = S_C + S_B = S_C + \ell_B = d_1 \sin\theta_{max}, \tag{B.17}$$

which is the maximum possible concentration.

3. Examples of Concentrators

In discussing some simple examples of the present design, we note that the case of circular cross section and unit concentration is the involute employed by Meinel and co-workers in their "cusp concentrator."[15] Moreover, the present scheme for concentrating onto a circular pipe has, in our understanding, been approached by their design.[16] Our construction for this case is shown in Fig. B.3.

An interesting example of our general design is shown in Fig. B.4 for a finlike receiver. In this case, the construction is a circle of radius W centered at P, extended by parabolas with foci at P. The concentration factor is

$$d_1/2W = 1/\sin\theta_{max}, \tag{B.18}$$

where the factor 2, in comparison with Eq. B.1, results from radiation illuminating both sides of the fin. This design could be used, for example, to illuminate both sides of a photovoltaic strip or both sides of an absorbing fin.

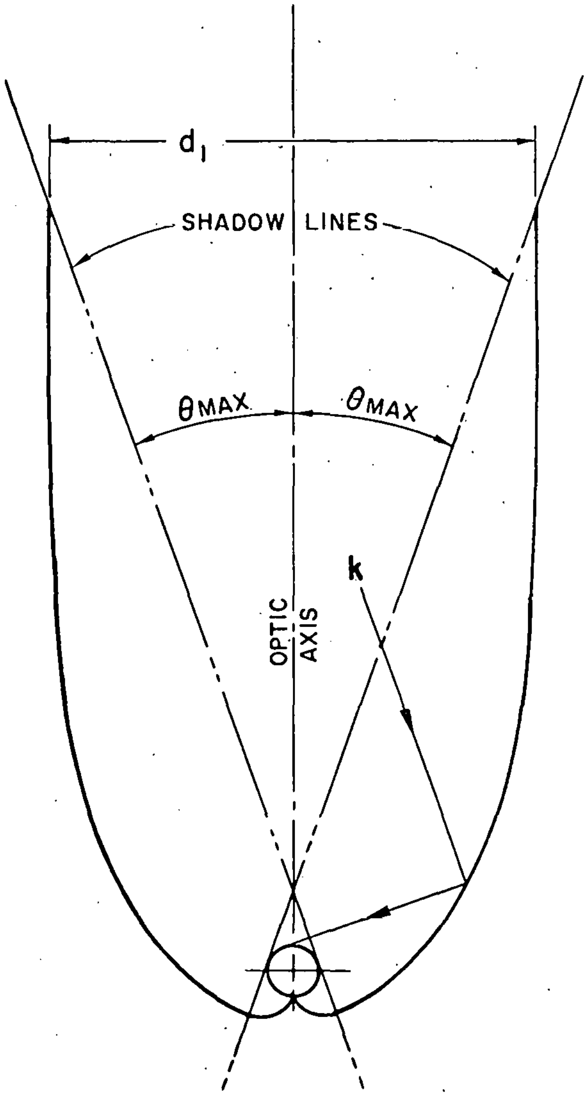

Fig. B.3. Profile Curve of X3 Concentrator for Circular Tube Receiver.

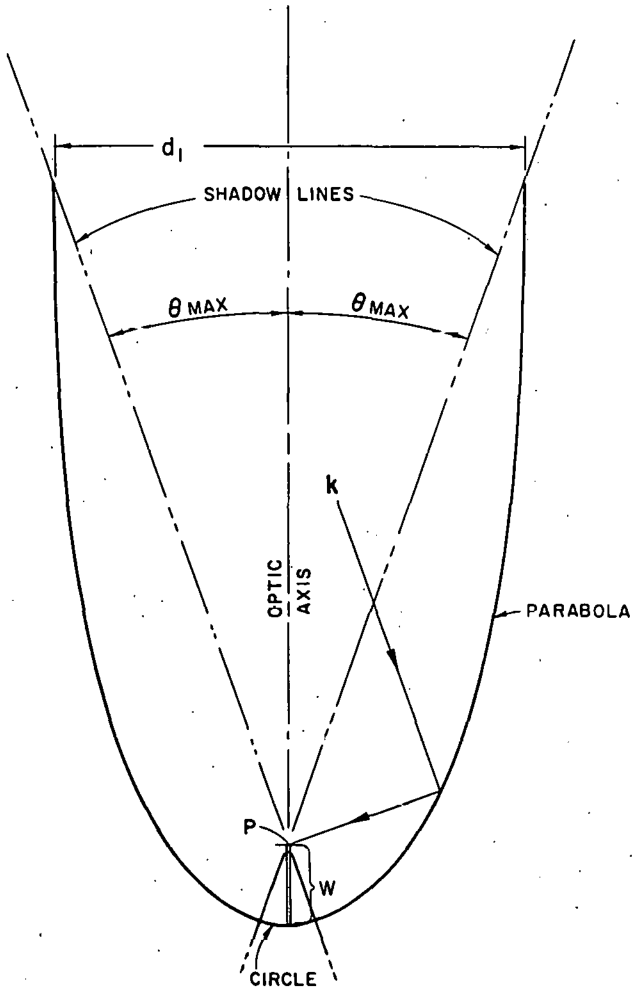

Fig. B.4. Profile Curve of X3 Concentrator for Fin Receiver.

It is apparent from the figures that concentrators of our design can be truncated substantially with very little loss of entrance aperture. This property is illustrated for the compound parabolic design (see Fig. 10). In most applications, truncated concentrators would be used on practical grounds. Note that truncation reduces concentration but not angular acceptance.

A characteristic property of our design is the small number of reflections when averaged over the angular acceptance. This is plausible, since rays incident at large angles $\theta \lesssim \theta_{max}$ have at most one reflection. The average number of reflections has been calculated by A. Rabl (see Sec. III) using an elegant analytic technique. The result for the compound parabolic case is shown in Fig. 12.

4. Conclusion

We have given a prescription for designing a cylindrical mirror to concentrate radiation onto a tube of general shape. The concentration factor, appropriately defined, is $1/\sin\theta_{max}$, which is the maximum possible. Unlike the parabolic case, this design is not applicable to rotationally symmetric (cone-shaped) mirrors. For certain applications involving specific receiver configurations, the present design may offer advantages over the compound parabolic cylindrical mirror proposed in Ref. 1.

APPENDIX C

List of Research Contributors

Argonne National Laboratory

R. Giugler
J. H. Martin
A. Rabl
V. Sevcik
R. Winston

University of Chicago

T. Sullivan (student)
R. Winston

Consultants

J. F. Kreider, Environmental Consulting Services, Inc.

APPENDIX D

List of Publications Resulting from Grant

Paper Accepted for Publication:

R. Winston and H. Hinterberger, "Principles of Cylindrical Concentrators for Solar Energy," Solar Energy (to be published).

Paper Submitted for Publication:

A. Rabl, "Optical and Thermal Properties of Compound Parabolic Concentrators."

REFERENCES

1. R. Winston, *Solar Concentrators of a Novel Design*, Solar Energy 16, 89 (1974).

2. V. J. Sevcik, R. M. Giugler, J. H. Martin, R. C. Neimann, A. Rabl and R. Winston, *Int. Solar Energy Soc.*, Fort Collins, Colo. (Aug 1974).

3. R. Winston, *Light Collection Within the Framework of Geometrical Optics*, J. Op. Soc. Am. 60, 245 (1970).

4. A. Rabl, *Comparison of Solar Concentrators*, ANL-SOL 75-02 (Apr 1975).

5. H. Hinterberger and R. Winston, *Efficient Light Coupler for Threshold Cerenkov Counters*, Rev. Sci. Instr. 37, 1094 (1966).

6. H. Hinterberger and R. Winston, Rev. Sci. Inst. 39, 1217 (1968).

7. A. Rabl, *Optical and Thermal Properties of Compound Parabolic Concentrators*, to be published in Solar Energy.

8. E. M. Sparrow and R. D. Cess, *Radiation Heat Transfer*, Brooks/Cole Publishing Co., Belmont, CA, p. 135 (Rev. Ed. 1970) (Hottel's string method).

9. A. Rabl, *Radiation Transfer Through Specular Passages*, ANL-SOL 75-03 (May 1975).

10. F. Kreith, *Principles of Heat Transfer*, 3rd Ed., Intext Educational Publishers, New York and London, (1973).

11. R. Winston, Enrico Fermi Institute Paper No. 72-21, Univ. of Chicago (1974).

12. W. H. McAdams, Heat Transmission, McGraw-Hill, New York (1953).

13. R. Siegel and J. R. Howell, *Thermal Radiation Heat Transfer*, McGraw-Hill, New York (1972).

14. C. G. Stokes, Proc. Roy. Soc. London 11, 545 (1860-62).

15. Presented by D. B. McKenney at National Science Foundation Solar Thermal Review (Mar 1974).

16. Private communication with A. B. Meinel, University of Arizona.